PCP
PLANT & CELL PHYSIOLOGY

Regular Paper

Alterations in Detergent-Resistant Plasma Membrane Microdomains in *Arabidopsis thaliana* During Cold Acclimation

Anzu Minami[1], Masayuki Fujiwara[2], Akari Furuto[3], Yoichiro Fukao[2], Tetsuro Yamashita[4], Masaharu Kamo[5], Yukio Kawamura[1] and Matsuo Uemura[1,3,*]

[1]The 21st Century Center of Excellence Program, Iwate University, Morioka, 020-8550 Japan
[2]Laboratory of Plant Molecular and Plant Protein Analysis, Plant Science Education Unit, Graduate School of Biological Sciences, Nara Institute of Science and Technology, Ikoma, 630-0101 Japan
[3]Cryobiofrontier Research Center, Faculty of Agriculture, Iwate University, Morioka, 020-8550 Japan
[4]Department of Biological Chemistry and Food Sciences, Faculty of Agriculture, Iwate University, Morioka, 020-8550 Japan
[5]Department of Biochemistry, Iwate Medical University School of Dentistry, Morioka, 020-8505 Japan

Microdomains in the plasma membrane (PM) have been proposed to be involved in many important cellular events in plant cells. To understand the role of PM microdomains in plant cold acclimation, we isolated the microdomains as detergent-resistant plasma membrane fractions (DRMs) from *Arabidopsis* seedlings and compared lipid and protein compositions before and after cold acclimation. The DRM was enriched in sterols and glucocerebrosides, and the proportion of free sterols in the DRM increased after cold acclimation. The protein-to-lipid ratio in the DRM was greater than that in the total PM fraction. The protein amount recovered in DRMs decreased gradually during cold acclimation. Cold acclimation further resulted in quantitative changes in DRM protein profiles. Subsequent mass spectrometry and Western blot analyses revealed that P-type H^+-ATPases, aquaporins and endocytosis-related proteins increased and, conversely, tubulins, actins and V-type H^+-ATPase subunits decreased in DRMs during cold acclimation. Functional categorization of cold-responsive proteins in DRMs suggests that plant PM microdomains function as platforms of membrane transport, membrane trafficking and cytoskeleton interaction. These comprehensive changes in microdomains may be associated with cold acclimation of *Arabidopsis*.

Keywords: *Arabidopsis* • Cold acclimation • Detergent-resistant membrane • 2D-DIGE • Microdomains • Plasma membrane.

Abbreviations: ASG, acylated sterylglucoside; BSA, bovine serum albumin; 2D-DIGE, two-dimensional difference gel electrophoresis; DRM, detergent-resistant plasma membrane fraction; DTT, dithiothreitol; GlcCer, glucocerebroside; FS, free sterol; LC-MS/MS, liquid chromatography-mass spectrometry/mass spectrometry; MALDI-TOF MS, matrix-assisted laser desorption/ionization time-of-flight mass spectrometry; PLD, phospholipase D; PL, phospholipid; PM, plasma membrane; P-ATPase, P-type H^+-ATPase; SG, sterylglucoside; TLC, thin-layer chromatography; V-ATPase, V-type H^+-ATPase

Introduction

Many plants increase tolerance to freezing stress when exposed to a non-freezing, low temperature for a certain period (Levitt 1980), a process known as cold acclimation. Cold acclimation results in physiological, morphological and molecular biological changes in plant cells (Guy 1990, Sharma et al. 2005). In many cases, upon freezing, ice formation occurs extracellularly and plant cells must keep ice out of the cytoplasm. Because the plasma membrane (PM) plays a central role in water transport into the cell and functions as a barrier to separate the cytoplasm from the extracellular region, it is generally thought that stabilization of the PM is a prerequisite for survival under freezing stress (Webb et al. 1994, Uemura et al. 2006).

*Corresponding author: E-mail, uemura@iwate-u.ac.jp; Fax, +81-19-621-6253.

Plant Cell Physiol. 50(2): 341–359 (2009) doi:10.1093/pcp/pcn202, available online at www.pcp.oxfordjournals.org

During cold acclimation, freezing tolerance of *Arabidopsis thaliana* is rapidly enhanced (Gilmour and Thomashow 1991), and this increase is associated with dynamic changes in protein and lipid compositions in the PM (Uemura et al. 1995, Kawamura and Uemura 2003). In addition, it has been reported that phospholipase D (PLD) associated with the PM increased during cold acclimation and, in fact, PLDδ-null mutants had less freezing tolerance than the wild type (Li et al. 2004). In contrast, freezing tolerance of antisense plant lines of PLDα1 increased (Welti et al. 2002), suggesting that PLDδ and PLDα signaling is mediated by different pathways. Cold acclimation resulted in rigidification of the PM, leading to depolymerziation of the cytoskeleton or activation of Ca^{2+} channels associated with the PM (Mazars et al. 1997, Orvar et al. 2000, Sangwan et al. 2001).

Cold acclimation results in a decrease in the proportion of a sphingolipid, glucocerebroside (GlcCer), in the PM of several plant species (Lynch and Steponkus 1987, Uemura et al. 1995). The effects of decreased GlcCer on freezing tolerance have been explained by temperature-dependent lipid physical properties. Exposure to low temperature results in a decrease in the PM fluidity and sometimes induces membrane lipid phase separation into crystalline and gel phases. Because GlcCer, a high melting-temperature lipid (Cahoon and Lynch 1991), tends to decrease membrane fluidity, the cold-induced decrease of GlcCer in the PM may increase membrane fluidity and affect survival at low temperatures (Steponkus et al. 1993).

A new concept for the role of sphingolipids in the PM, 'membrane microdomains' (also known as 'membrane/lipid rafts' in some cases), has been proposed in animals and microorganisms. The membrane microdomain concept assumes that membrane lipids and proteins move unevenly and are distributed non-uniformly in the membrane (Kusumi et al. 2005, Lillemeier et al. 2006). This uneven distribution of membrane components is considered to be dependent on sphingolipids and sterols. Sphingolipids have the feature of easily self-associating in the PM through long saturated acyl chains (Thompson and Tillack 1985). Hence, sphingolipids tend to exist as microdomains in association with sterols and are localized differently from other lipids in the PM (Simons and Ikonen 1997). This microdomain model has been supported by analysis of visualization of membrane components on cell surfaces (Simons and Toomre 2000).

Because sphingolipids and sterols are more resistant than phospholipids (PLs) to detergent extraction (Schroeder et al. 1994), sphingolipid- and sterol-enriched microdomains are obtained as detergent-resistant membrane fractions (DRMs) from isolated PM preparations. In animal cells, the DRM contains specific proteins, such as receptor proteins, kinases, G-proteins and syntaxins, suggesting association with signal transduction, membrane trafficking or pathogen infection (Brown and London 1998, Rajendran and Simons 2005). The stomatin/prohibitin/flotillin/HlfK/C (SPFH) protein family is also associated with membrane/lipid rafts (Salzer and Prohaska 2001, Langhorst et al. 2005). The protein family acts as scaffolding proteins that recruit signaling proteins into the membrane/lipid rafts (Nadimpalli et al. 2000, Langhorst et al. 2005). Using single particle tracking and fluorescence resonance energy transfer techniques, the microdomains on the PM have been estimated to be ≤200 nm in diameter, but, interestingly, the size dynamically changes during signaling (Anderson and Jacobson 2002).

Recently, plant DRMs were isolated and their protein and lipid compositions were analyzed. The proportions of both sphingolipids and sterols are greater in the DRM than in the total PM (Berczi and Horvath 2003, Mongrand et al. 2004, Borner et al. 2005, Laloi et al. 2007, Lefebvre et al. 2007). Proteomic analysis suggested that plant DRMs are involved in signal transduction, membrane trafficking and cell wall metabolism occurring on the PM (Peskan et al. 2000, Mongrand et al. 2004, Shahollari et al. 2004, Bhat and Panstruga 2005, Borner et al. 2005, Morel et al. 2006, Laloi et al. 2007, Lefebvre et al. 2007). These results are consistent with those in DRMs of animal and microorganism cells. Furthermore, Bhat et al. (2005) showed that two PM proteins, MLO and ROR2 (a syntaxin), accumulated at sterol-enriched pathogen entry sites in barley epidermal cells, suggesting that DRMs work as a platform for pathogen entry into a host plant cell. In addition, some proteins in DRMs have been proposed to function in endocytosis (Bloch et al. 2005, Yalovsky et al. 2008) and fungus-mediated growth promotion (Shahollari et al. 2007). Nevertheless, the function of microdomains in the plant PM in abiotic stress responses has yet to be determined.

Because GlcCer and free sterols (FS) are likely to be involved in the formation of membrane microdomains and the proportion of these lipids alters in the PM during cold acclimation in plants, we hypothesized that GlcCer and FS not only affect membrane fluidity but also assemble into local domains in the PM during cold acclimation. Further, there may be a difference in changes in protein compositions in the DRM and the total PM. As a first step to examine our hypothesis, we investigated changes in lipid and protein compositions in DRMs before and after cold acclimation of *Arabidopsis* seedlings. We carried out quantitative lipid analysis by thin-layer chromatography (TLC) and determined the change in DRM lipid composition during cold acclimation. For identification of cold responsiveness in DRM proteins, we employed the fluorescence two-dimentional difference gel electrophoresis (2D-DIGE) technique, which is one of the powerful approaches for quantitative proteome analysis of plant DRMs (Borner et al. 2005). With our results, we further discuss a possibility of microdomain involvement in plant cold acclimation.

Results

Changes in DRM lipid composition during cold acclimation

Arabidopsis DRMs were visible as two white bands at 35–45% (w/w) sucrose concentrations after centrifugation. Because protein profiles after 2D-PAGE were similar in these bands (data not shown), the two bands were combined and designated as DRMs. **Table 1** shows the lipid composition of the PM and DRM from *Arabidopsis* seedlings. Both membrane samples contain sterols, GlcCer and PLs. Sterols were further classified as FS, acylated sterylglucosides (ASGs) and sterylglucosides (SGs). PLs were not completely separated in detail in the present study and were considered as a mixture of several classes of PLs.

The results in **Table 1** clearly showed that DRMs could be defined as sphingolipid- and sterol-enriched fractions when compared with the PM. In DRMs of non-acclimated samples, the proportions of GlcCer and sterols were 11.5 and 52.0 mol% of the total lipids, respectively, which were 2.6 and 1.6 times greater than those in the PM. For sterols, ASG and SG were considerably enriched in DRMs, but FS was not. Concomitantly, the proportion of PLs was much less in DRMs (36.6 mol%) than in the PM (63.8 mol%) of non-acclimated samples. When the amounts of lipid per mg of protein were compared, DRMs contained smaller amounts of lipids than did PM fractions, suggesting enrichment of proteins in DRMs.

Next, we compared lipid compositions of DRMs in non-acclimated and 7 d cold-acclimated samples (**Table 1**). Sterols in DRMs increased from 52.0 to 57.8 mol% of the total lipids during cold acclimation, but GlcCer and PLs did not increase. The increase in sterols was due to the increase in FS and ASGs. In fact, the amount of FS increased significantly after cold acclimation for 7 d from 411 to 505 nmol mg^{-1} proteins ($P < 0.05$). Though not statistically significant, the amounts of ASG and SG also increased (from 128 to 168 nmol mg^{-1} proteins and from 165 to 184 nmol mg^{-1} proteins). Consequently, the lipid-to-protein ratio in DRMs increased slightly after cold acclimation for 7 d (1,356 to 1,489 nmol lipids mg^{-1} proteins). Furthermore, the DRM/PM ratios of ASGs, SGs and GlcCer became much greater after cold acclimation, but those of FS and PLs did not change (**Fig. 1**).

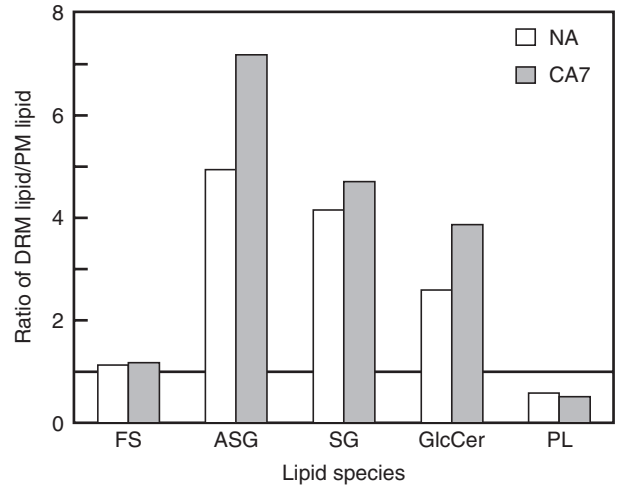

Fig. 1 Lipid compositions of the PM and DRM before and after cold acclimation. White bars, non-acclimated (NA); shaded bars, cold acclimated for 7 d (CA7). Lipid distribution was expressed as the ratio of mol% (of total lipids) of each lipid in the DRM to that in the total PM. FS, free sterols; ASG, acylated sterylglucosides; SG, sterylglucosides; GlcCer, glucocerebrosides; PL, phospholipids.

Changes in protein recovery in DRMs during cold acclimation

The amount of protein recovered in DRMs decreased gradually during cold acclimation (**Fig. 2**). In a non-acclimated sample, the protein recovery in DRMs was 9.5 ± 3.1% of that of the total PM. The recovery rate of protein in DRMs decreased

Table 1 Lipid compositions of PM and DRM [mol% of the total lipids (nmol mg^{-1} protein)] isolated from non-acclimated (NA) and 7 d cold-acclimated (CA7) *Arabidopsis* seedlings

Lipid	PM		DRM	
	NA ($n = 3$)	CA7 ($n = 3$)	NA ($n = 5$)	CA7 (n = 6)
Sterols	31.8 ± 1.2 (514 ± 56)	33.4 ± 2.0 (627 ± 74)	52.0 ± 4.3 (704 ± 99)	57.8 ± 3.8 (856 ± 48*)
FS	27.0 ± 0.5 (435 ± 37)	29.2 ± 2.1 (549 ± 69)	30.4 ± 3.2 (411 ± 52)	34.2 ± 3.8 (505 ± 35*)
ASG	1.9 ± 0.6 (30 ± 9)	1.6 ± 0.4 (29 ± 7)	9.3 ± 1.9 (128 ± 38)	11.3 ± 1.8 (168 ± 24)
SG	3.0 ± 0.7 (48 ± 16)	2.6 ± 1.0 (50 ± 19)	12.3 ± 1.4 (165 ± 21)	12.3 ± 0.3 (184 ± 22)
GlcCer	4.4 ± 1.2 (70 ± 16)	2.6 ± 1.1 (47 ± 18)	11.5 ± 7.0 (158 ± 102)	9.9 ± 3.6 (151 ± 64)
PL	63.8 ± 0.7 (1,027 ± 68)	64.1 ± 1.4 (1,199 ± 46*)	36.6 ± 3.0 (494 ± 61)	32.3 ± 2.9 (482 ± 73)
Total	100 (1,612 ± 111)	100 (1,874 ± 107)	100 (1,356 ± 162)	100 (1,489 ± 151)

ASG, acylated sterylglucosides; FS, free sterols; GlcCer, glucosylcerebrosides; PL, phospholipids; SG, sterylglucosides.
The results are means ± SE of 3–6 determinations.
*$P < 0.05$ by Student's *t*-test.

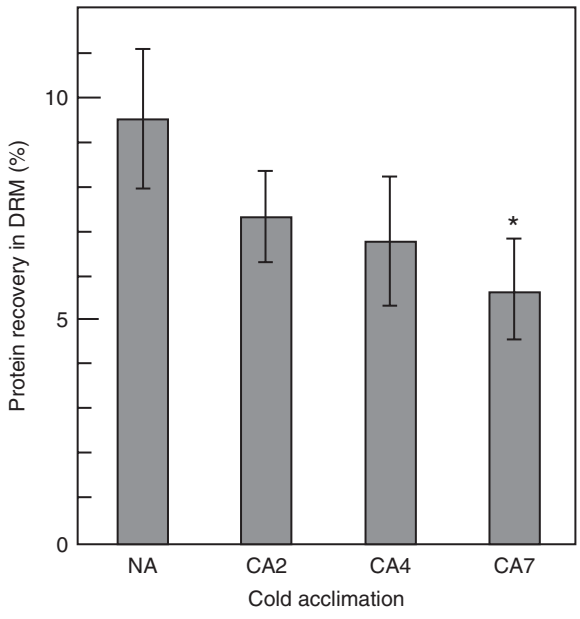

Fig. 2 Changes in the amount of protein recovered as DRMs during cold acclimation. NA, non-acclimated; CA2, CA4 and CA7, cold acclimated for 2, 4 and 7 d, respectively. Data are expressed as the proportion of proteins recovered in DRMs from the PM fractions. Data are means and SEs of 3–7 independent experiments. An asterisk indicates a significant difference from the non-acclimated sample (Student's *t*-test, $P < 0.05$).

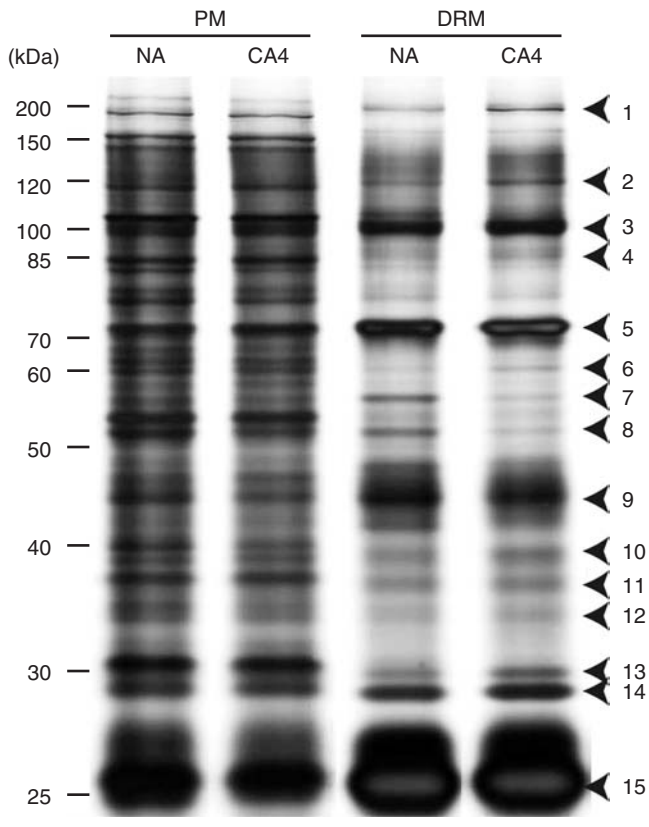

Fig. 3 SDS–PAGE profiles of PM and DRM proteins. NA, non-acclimated; CA4, cold acclimated for 4 d. Proteins (3 μg) were separated by 10% SDS–PAGE and then visualized with the silver staining method. Arrowheads indicate the identified proteins in DRMs (**Table 2**).

with the period of cold acclimation: 7.3 ± 2.0, 6.8 ± 2.5 and 5.7 ± 2.6% after cold acclimation for 2, 4 and 7 d, respectively. The recovery after cold acclimation for 7 d was statistically and significantly less than that of non-acclimation ($P < 0.05$).

SDS–PAGE profiles of DRM proteins before and after cold acclimation

Fig. 3 shows SDS–PAGE profiles of PM and DRM proteins prepared from non-acclimated and 4 d cold-acclimated plants. There were distinct differences in PM and DRM protein profiles, and the number of protein bands of DRMs seemed to be less than that of PM fractions, suggesting enrichment of specific proteins in the DRM. Furthermore, cold acclimation caused changes in many proteins in both DRMs and PM fractions.

With 15 bands from gels, we successfully identified 80 different proteins as DRM proteins using liquid chromatography-mass spectrometry/mass spectrometry (LC-MS/MS) and matrix-assisted laser desorption/ionization time-of-flight mass spectrometry (MALDI-TOF/MS) (**Table 2**). Among the identified DRM proteins were 28 membrane transport-related proteins, including P-type H^+-ATPases (P-ATPase) (10), aquaporins (10) and V-type H^+-ATPase (V-ATPase) subunits (five), 12 cytoskeleton-related proteins, including tubulins (11) and actins (two), and 10 vesicle trafficking-related proteins, including homologs of clathrins (three), dynamins (two) and synaptotagmins (two). In addition, there were protein kinases, microdomain-associated proteins and cell wall- and metabolism-related proteins in DRMs, which is consistent with the results in previous reports (Bhat and Panstruga 2005, Morel et al. 2006, Lefebvre et al. 2007). Furthermore, putative peripheral (with no putative transmembrane domains) and lipid-modified (proteins with a glycosylpho-sphatidylinositol anchor or a putative myristoylation site) proteins accounted for 51% (41 proteins) of the total identified DRM proteins.

2D-DIGE profiling of DRM proteins during cold acclimation

To analyze further peripheral or integral membrane proteins with one or two transmembrane domains (Bunai and Yamane 2005), we carried out 2D-DIGE of DRM proteins. 2D-DIGE is a technique for easy comparison of different samples separated on the same gel using three different fluorescent dyes (see Materials and Methods; Marouga et al. 2005).

Table 2 MALDI-TOF/MS and LC-MS/MS identification of DRM proteins in *Arabidopsis* separated by SDS–PAGE

No.	Exp. MM[a] (kDa)	Protein name[b]	Theo. MM[c] (D/pI)	Accession No.	AGI code No.	TM[d]	MASCOT score[e] (matched peptide)	MOWSE score[f]	Category[g]
1	184.6	AHA1 (P-type H$^+$-ATPase)	104,225/6.7	P20649	At2g18960	9	289 (20)		1
		AHA2 (P-type H$^+$-ATPase)	104,403/7.0	P19456	At4g30190	9	284 (18)		1
		Clathrin heavy chain	193,243/5.1	Q0WNJ6	At3g11130	0	183 (9)		2
		Clathrin heavy chain, 3′ partial	193,273/5.0	Q0WLB5	At3g08530	0	145 (7)		2
		PDR8 (ABC transporter)	165,081/8.0	Q9XIE2	At1g59870	11	67 (3)		1
		AHA11 (P-type H$^+$-ATPase)	105,122/6.6	Q9LV11	At5g62670	10	65 (4)		1
		AHA5 (P-type H$^+$-ATPase)	102,661/7.6	Q9SJB3	At2g24520	9	60 (4)		1
		AHA9 (P-type H$^+$-ATPase)	105,207/6.3	Q42556	At1g80660	10	59 (4)		1
		AHA7 (P-type H$^+$-ATPase)	105,505/6.8	Q9LY32	At3g60330	9	40 (2)		1
		CALS9 (callose synthase 9)	222,089/8.7	Q9SFU6	At3g07160	14	39 (1)		5
2	115.6	AHA1 (P-type H$^+$-ATPase)	104,225/6.7	P20649	At2g18960	9	138 (10)		1
		AHA11 (P-type H$^+$-ATPase)	105,122/6.6	Q9LV11	At5g62670	10	102 (4)		1
		AHA9 (P-type H$^+$-ATPase)	105,207/6.3	Q42556	At1g80660	10	64 (6)		1
3	102.1	AHA1 (P-type H$^+$-ATPase)	104,225/6.7	P20649	At2g18960	9	409 (9)		1
		AHA2 (P-type H$^+$-ATPase)	104,403/7.0	P19456	At4g30190	9	380 (8)		1
		AHA6 (P-type H$^+$-ATPase)	105,014/6.1	Q9SH76	At2g07560	10	270 (5)		1
		AHA11 (P-type H$^+$-ATPase)	105,122/6.6	Q9LV11	At5g62670	10	181(4)		1
		AHA4 (P-type H$^+$-ATPase)	105,717/6.5	Q9SU58	At3g47950	10	181(4)		1
		AHA5 (P-type H$^+$-ATPase)	102,661/7.6	Q9SJB3	At2g24520	9	107 (3)		1
		AHA10 (P-type H$^+$-ATPase)	104,814/6.4	Q43128	At1g17260	9	96 (4)		1
		AHA9 (P-type H$^+$-ATPase)	105,207/6.3	Q42556	At1g80660	10	93(6)		1
		VHA-a3 (V-type H$^+$-ATPase subunit a3)	92,833/5.8	Q8W4S4	AT4g39080	5	89(5)		1
		TPR repeat-containing protein	90,169/6.7	O23052	At1g05150	0	52 (2)		7
		TPR repeat-containing protein	90,228/6.7	Q8S8L9	At2g32450	0	52 (2)		7
		AHA7 (P-type H$^+$-ATPase)	105,505/6.8	Q9LY32	At3g60330	9	47(3)		1
4	84.4	AHA1 (P-type H$^+$-ATPase)	104,225/6.7	P20649	At2g18960	9	155(13)		1
		AHA2 (P-type H$^+$-ATPase)	104,403/7.0	P19456	At4g30190	9	154 (13)		1
		AHA11 (P-type H$^+$-ATPase)	105,122/6.6	Q9LV11	At5g62670	10	131 (7)		1
		AHA10 (P-type H$^+$-ATPase)	104,814/6.4	Q43128	At1g17260	9	104 (5)		1
		AHA9 (P-type H$^+$-ATPase)	105,207/6.3	Q42556	At1g80660	10	96 (3)		1
		SKU5 (putative monocopper oxidase precursor)	65,638/9.5	Q9SU40	At4g12420	1 (GPI)	96 (2)		5
		AHA8 (P-type H$^+$-ATPase)	104,130/5.5	Q9M2A0	At3g42640	10	92 (6)		1
		Receptor lectin protein kinase	75,541/8.0	O80939	At2g37710	3	88 (4)		6
		Delta-1-pyrroline-5-carboxylate synthetase B	78,871/6.8	P54888	At3g55610	0	80 (2)		7
		Lectin protein kinase	77,599/6.9	Q9SR87	At3g08870	0 (M)	62 (2)		6
		Protein kinase	75,554/8.8	O64639	At2g45590	1	62 (1)		6
5	70.4	ERD4*	81,936/9.6	Q9C8G5	At1g30360	10	531 (31)	1.93E + 26	7
		VHA-A (V-type H$^+$-ATPase subunit A)	68,813/5.1	O23654	At1g78900	0	149 (9)		1
		DRP1A (dynamin-related protein)	68,173/8.5	P42697	At5g42080	0	98 (3)		2
		DRP1E (dynamin-related protein)	69,804/7.2	Q9FNX5	At3g60190	0	24 (1)		2
6	59.6	ERD4	81,936/9.6	Q9C8G5	At1g30360	10	313 (17)		7
		STP1 (sugar transporter)	57,610/9.2	P23586	At1g11260	11	112 (2)		1
		SYT1 (synaptotagmin homolog)	61,744/7.7	Q9SKR2	At2g20990	1	102 (5)		2

continued

Table 2 Continued

No.	Exp. MM[a] (kDa)	Protein name[b]	Theo. MM[c] (D/pI)	Accession No.	AGI code No.	TM[d]	MASCOT score[e] (matched peptide)	MOWSE score[f]	Category[g]
		PIRL4 (leucine-rich repeat protein)	60,994/5.3	Q9SVW8	At4g35470	0	86(4)		7
		TUA6 (tubulin α-6 chain)	49,538/4.7	P29511	At4g14960	0	59 (1)		3
		TUA3 (tubulin α-3/α-5 chain)	49,654/4.7	P20363	At5g19770/ At5g19780	0	59 (1)		3
		TUA2 (tubulin α-2/α-4 chain)	49,541/4.7	P29510	At1g04820/ At1g50010	0	59 (1)		3
		SYT5 (synaptotagmin homolog)	62,928/5.6	Q8L706	At1g05500	2	52 (4)		2
		STP13 (sugar transporter)	57,419/9.0	Q94AZ2	At5g26340	11	48 (1)		1
7	55.9	VHA-B2 (V-type H^+-ATPase subunit B2)	54,306/4.8	Q9SZN1	At4g38510	0	351 (16)		1
		VHA-B3 (V-type H^+-ATPase subunit B3)	54,255/4.9	Q8W4E2	At1g20260	0	350 (16)		1
		TUB2 (tubulin β2/β-3 chain)	50,735/4.4	P29512	At5g62690/ At5g62700	0	99 (3)		3
		TUB5 (tubulin β-5 chain)	50,342/4.4	P29513	At1g20010	0	99 (3)		3
		TUB9 (tubulin β-9 chain)	49,659/4.4	P29517	At4g20890	0	99 (3)		3
		CaLB (calcium/lipid-binding protein)	55,095/8.6	Q9LEX1	At3g61050	1	71 (1)		7
8	51.8	TUB6 (tubulin β-6 chain)*	50,586/4.4	P29514	At5g12250	0	–	2.39E + 11	3
		TUB4 (tubulin β-4 chain)	49,823/4.5	P24636	At5g44340	0	194 (8)		3
		TUA6 (tubulin α-6 chain)	49,538/4.7	P29511	At4g14960	0	193 (7)		3
		PIP2B (aquaporin)	30,453/8.0	P43287	At2g37170	5	180 (12)		1
		PIP2A (aquaporin)	30,474/8.6	P43286	At3g53420	5	158 (13)		1
		TUB2 (tubulin β-2/β-3 chain)	50,735/4.4	P29512	At5g62690/ At5g62700	0	146 (7)		3
		TUB5 (tubulin β-5 chain)	50,342/4.4	P29513	At1g20010	0	142 (5)		3
		TUA3 (tubulin α-3/α-5 chain)	49,654/4.7	P20363	At5g19770/ At5g19780	0	137 (7)		3
		TUB7 (tubulin β-7 chain)	50,747/4.5	P29515	At2g29550	0	117 (5)		3
		TUB8 (tubulin β-8 chain)	50,607/4.5	P29516	At5g23860	0	97 (4)		3
		PIP1B (aquaporin)	32,455/8.6	Q06611	At2g45960	6	95 (4)		1
		TUA1 (tubulin α-1 chain)	49,800/4.7	P11139	At1g64740	0	85 (2)		3
		CaLB (calcium/lipid-binding protein)	55,095/8.6	Q9LEX1	At3g61050	1	79 (3)		7
		Band 7 family protein	31,321/5.5	Q9SRH6	At3g01290	0 (M)	65 (3)		4
		PIP3 (aquaporin)	29,742/9.1	P93004	At4g35100	4	64 (4)		1
		eEF-1A (elongation factor 1-α)	49,503/9.2	P13905	At1g07940/ At1g07920/ At1g07930/ At5g60390	0	63 (6)		5
		Clathrin light chain	37,225/6.1	Q9SKU1	At2g20760	0	53 (2)		2
		Pentatricopeptide repeat containing protein	66,325/7.9	Q9SN85	At3g47530	0	41 (1)		7
9	44.8	PIP2A (aquaporin)	30,474/8.6	P43286	At3g53420	5	101 (7)		1
		PIP2B (aquaporin)	30,453/8.0	P43287	At2g37170	5	77 (4)		1
		ACT7 (actin-7)	41,735/5.2	P53492	At5g09810	0	77 (3)		3
		Putative uncharacterized protein	34,732/10.0	Q9C9Z6	At3g08600	2	72 (4)		7
		ACT8 (actin-8)	41,863/5.3	Q96293	At1g49240	0	72 (1)		3
		PIP1B (aquaporin)	32,455/8.6	Q06611	At2g45960	6	68 (4)		1

Continued

Table 2 Continued

No.	Exp. MM[a] (kDa)	Protein name[b]	Theo. MM[c] (D/pI)	Accession No.	AGI code No.	TM[d]	MASCOT score[e] (matched peptide)	MOWSE score[f]	Category[g]
		PIP3 (aquaporin)	29,742/9.1	P93004	At4g35100	4	52 (3)		1
		F-box/FBD/LRR protein	53,865/5.8	Q9FNK0	At5g22610	0	46 (1)		7
		PIP2C (aquaporin)	30,429/8.0	P30302	At2g37180	5	46 (2)		1
		PIP1D (aquaporin)	30,646/9.1	Q8LAA6	At4g23400	5	43 (1)		1
		Epsin3 (clathrin-binding protein)	30,800/9.3	Q9ZW79	At2g43160	0	42 (1)		2
10	38.8	Leucine-rich repeat protein kinase	67,463/8.7	Q9FMD7	At5g16590	2	46 (1)		6
		Protein kinase	39,562/9.1	Q9LUT0	At3g17410	0 (M)	45 (1)		6
11	36.2	Remorin family protein	23,144/5.3	Q9M2D8	At3g61260	0	336 (16)		4
		NDR1/HIN1-like protein 3 (harpin-induced 3)	25,947/9.5	Q9FNH6	At5g06320	2	96 (3)		7
		Harpin-induced 1	25,784/10.5	Q8LE22	At3g54200	1	77(1)		7
		Endomembrane-associated protein	24,569/5.0	Q2L6T2	At4g20260	0	48 (4)		7
12	33.6	Band 7 family protein	31,406/5.1	Q9CAR7	At1g69840	0	256 (11)		4
		NDR1/HIN1-like protein 3 (harpin-induced 3)	25,947/9.5	Q9FNH6	At5g06320	2	174 (4)		7
		Remorin family protein	20,968/9.0	O80837	At2g45820	0	138 (11)		4
		PIP2A (aquaporin)	30,474/8.6	P43286	At3g53420	5	80 (3)		1
		Band 7 family protein	31,321/5.5	Q9SRH6	At3g01290	0 (M)	75 (3)		4
		Unknown protein	28,288/10.7	Q9LNP3	At1g17620	1	53 (1)		7
		Unknown protein	27,087/9.2	Q8VZ18	At3g44150	0	43 (1)		7
		Snf7	25,292/5.3	Q9SKI2	At2g06530	0	34 (1)		2
13	29.5	Band 7 family protein*	31,406/5.1	Q9CAR7	At1g69840	0	390 (17)	2.17E + 26	4
		Band 7 family protein	31,431/5.1	Q9FM19	At5g62740	0 (M)	124 (6)		4
		ThiF family protein	50,559/6.1	Q08A97	At5g37530	2	39 (2)		7
		Band 7 family protein	31,321/5.5	Q9SRH6	At3g01290	0 (M)	32 (4)		4
14	28.8	Band 7 family protein*	31,321/5.5	Q9SRH6	At3g01290	0 (M)	720 (56)	2.37E + 15	4
		Band 7 family protein	31,431/5.1	Q9FM19	At5g62740	0 (M)	307 (13)		4
		Band 7 family protein	31,406/5.1	Q9CAR7	At1g69840	0	70 (2)		4
		SYP71 (syntaxin-71)	29,983/4.8	Q9SF29	At3g09740	1	53 (4)		2
15	25.1	PIP2A (aquaporin)	30,474/8.6	P43286	At3g53420	5	127 (4)		1
		PIP1B (aquaporin)	32,455/8.6	Q06611	At2g45960	6	122 (6)		1
		PIP1D (aquaporin)	30,646/9.1	Q8LAA6	At4g23400	5	105 (3)		1
		PIP1A (aquaporin)	30,688/9.3	P61837	At3g61430	6	87 (4)		1
		PIP2D (aquaporin)	30,589/9.0	Q9SV31	At3g54820	6	69 (2)		1
		PIP2E (aquaporin)	31,050/8.3	Q9ZV07	At2g39010	5	59 (3)		1
		Oxidoreductase	34,417/9.5	Q3E6X4	At1g73650	7	58 (1)		5
		PIP3 (aquaporin)	29,742/9.1	P93004	At4g35100	4	53(3)		1
		PIP1E (aquaporin)	30,693/9.1	Q39196	At4g00430	6	73 (2)		1

[a]Exp. MM, experimentally obtained molecular mass.
[b]Asterisks indicate proteins identified by MALDI-TOF/MS.
[c]Theo. MM, theoretical molecular mass determined from the database.
[d]TM, putative transmembrane domains predicted by SOSUI. GPI, glycosylphosphatidylinositol-anchored protein confirmed by Sedbrook et al. (2002). M, putative myristoylation site.
[e]MASCOT scores of proteins identified by LC-MS/MS are listed. The number in parentheses indicates the number of matched peptides
[f]MOWSE scores of proteins identified by MALDI-TOF/MS are listed.
[g]Category, predicted function of proteins were categorized into (1) membrane transport, (2) vesicle trafficking, (3) cytoskeleton, (4) microdomain-associated proteins, (5) plasma membrane and cell wall reconstruction, (6) signal transduction, and (7) others.

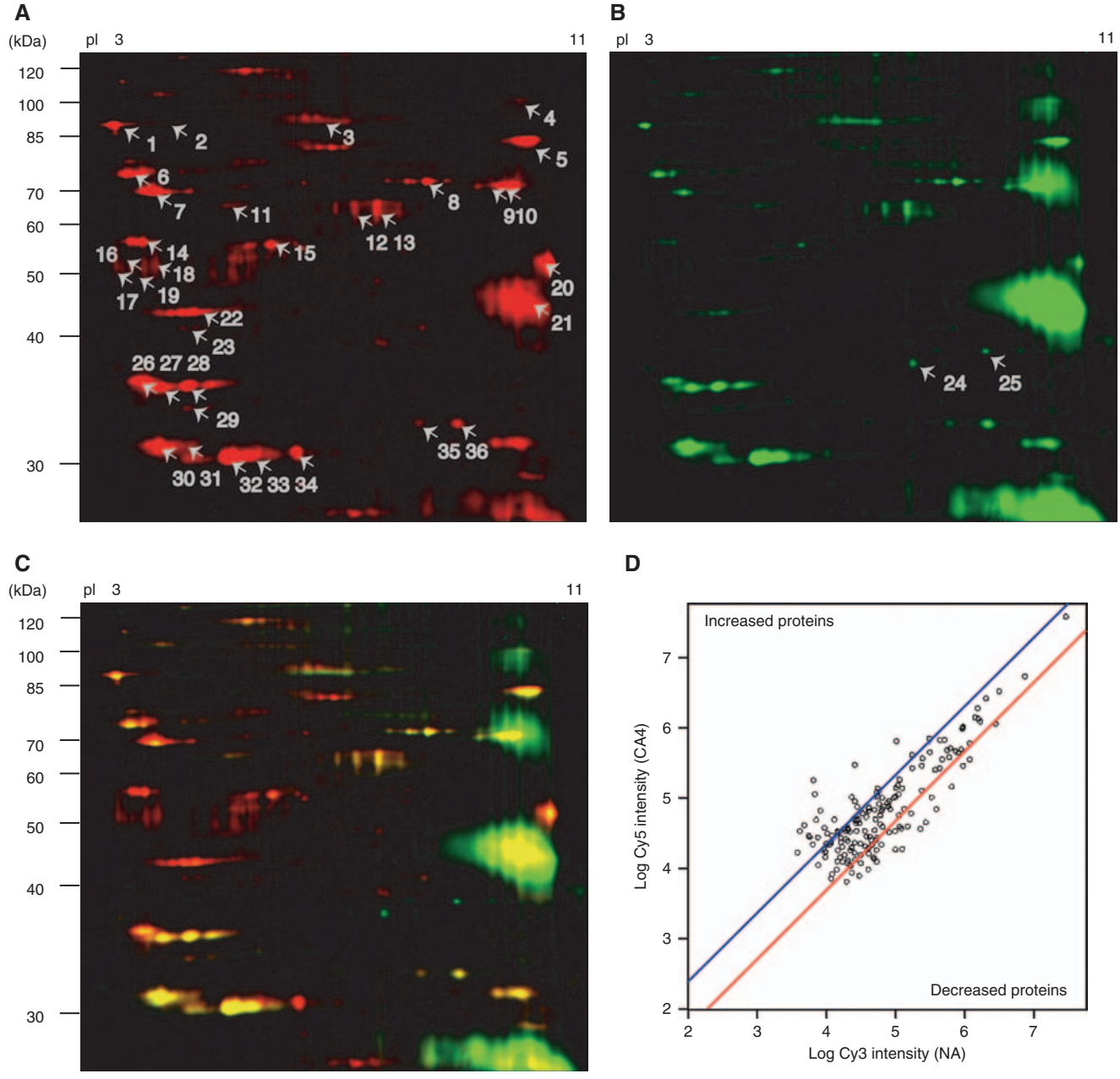

Fig. 4 (A) 2D-DIGE profiles of DRM proteins. DRM proteins labeled with Cy dye were separated by 2D-DIGE. (A) Proteins in non-acclimated DRM labeled with Cy3; (B) proteins in 4 d cold-acclimated DRM labeled with Cy5; (C) false color overlay of proteins in non-acclimated (red) and 4 d cold-acclimated (green) DRMs. (D) Relationship of accumulation levels of proteins in non-acclimated (NA) and 4 d cold-acclimated (CA4) DRMs. The normalized fluorescence intensity of 165 major DRM proteins was plotted. The quantity of each spot of the NA sample (*x*-axis) is plotted against that of the CA4 sample (*y*-axis). Two parallel lines in the panel indicate a 2-fold increase (blue) or 0.5-fold decrease (red) in expression ratios after cold acclimation for 4 d. Spot numbers on the gel (A and B) correspond to those in **Table 4**.

Fig. 4A and **B** shows examples of 2D-DIGE patterns of DRM proteins isolated from non-acclimated (NA, Cy3-labeled) and 4 d cold-acclimated (CA4, Cy5-labeled) plants, respectively. When the two images taken from the same gel were overlaid (**Fig. 4C**), there were many green spots and red spots that indicate that proteins increased and decreased during cold acclimation, respectively. Spots with yellow color indicate that the extent of change during cold acclimation was relatively small. In general, DRM proteins with acidic pIs seemed to decrease after cold acclimation, whereas proteins with basic pIs increased.

Table 3 Number of DRM proteins during cold acclimation in *Arabidopsis*

	NA-CA2	NA-CA4	NA-CA7	CA2-CA4	CA4-CA7
> 2-fold increase	31	31	35	31	17
< 0.5-fold decrease	29	28	32	21	18
Unchanged	105	106	98	113	130
Total	165	165	165	165	165

The number of cold-increased or cold-decreased proteins determined at two points during CA is shown. NA, CA2, CA4 and CA7 indicate non-acclimated and cold acclimated for 2, 4 and 7 d, respectively. For reference, the number of unchanged proteins is also included. NA-CA2, changes from NA to 2 d CA samples; NA-CA4, changes from NA to 4 d CA samples; NA-CA7, changes from NA to 7 d CA samples; CA2-CA4, changes from 2 d CA to 4 d CA samples, CA4-CA7, changes from 4 d CA to 7 d CA samples.

Changes in DRM proteins during cold acclimation were quantitatively analyzed by the fluorescence intensity of each protein spot in two samples prepared at different times of cold acclimation (**Fig. 4D** and **Table 3**). A total of 165 protein spots was detected and matched on all 2D-DIGE gel images analyzed. When a cut-off of >2 or <0.5 in the fluorescence ratio of the spot between the two samples was applied, we found, for example, that there were 31 increased proteins and 29 decreased proteins during the first 2 d of cold acclimation (NA vs. CA2). Although the number of proteins responding to cold acclimation fluctuated somewhat in each comparison, many proteins in DRMs (20 to 40%) changed quantitatively during cold acclimation.

Next, we selected 36 protein spots from 2D-PAGE gels (**Fig. 4A, B**) and performed LC-MS/MS and/or MALDI-TOF/MS analyses for protein identification (**Table 4**). As predicted, we identified many peripheral membrane proteins in DRMs. Spot 6 matched Hsc70s [Hsc70.1 (P22953), Hsc70.2 (P22954) and Hsc70.3 (O65719)] in the MS-Fit database. The three Hsc70s have high amino acid similarity to each other (> 92%). Likewise, spot 19 matched TUA2 and TUA6, and spot 22 matched ACT8 and ACT2. For some DRM proteins, molecular weights determined on the gels were inconsistent with the predicted molecular weights: e.g. patellin-1 (#1) was detected with an apparent molecular mass of 97.1 kDa on a 2D-PAGE gel, while the predicted molecular mass is 64 kDa; and SKU5 (#5) with a predicted mass of 65.6 kDa was detected on an SDS–PAGE gel at 80.1 kDa. This is probably due to the existence of an acidic N-terminal domain in the protein, which causes unpredictable mobility on the gel (Peterman et al. 2004), or post-translational modification (Sedbrook et al. 2002). A spot of a basic protein that appeared at 42.6 kDa (#21) was identified as aquaporin, which may be a dimeric form based on information on its molecular weight.

Changes of the 36 identified proteins during cold acclimation were next analyzed statistically with Student's *t*-test and were categorized into three groups (**Fig. 5** and **Supplementary Table S1**): increased (>2-fold change), decreased (<0.5-fold change) and unchanged proteins (between 0.5- and 2-fold change). Three protein spots (#2, 3 and 21) could not

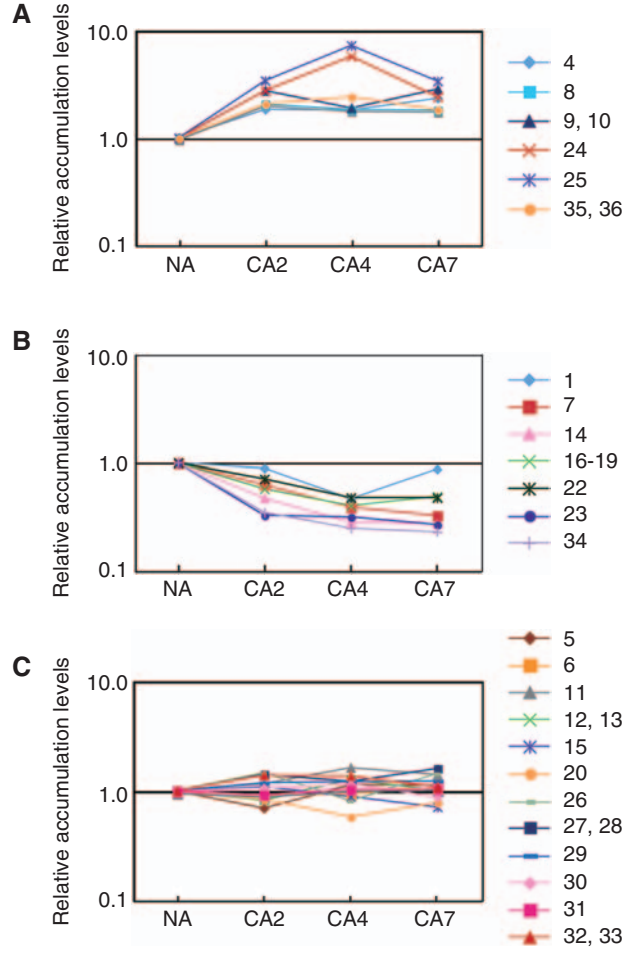

Fig. 5 Categorization of the responsiveness of DRM proteins to cold. NA, non-acclimated; CA2, CA4 and CA7, cold acclimated for 2, 4 and 7 d, respectively. The ratio of the fluorescence intensity of DRM proteins of cold-acclimated to non-acclimated samples was calculated using PDQuest V 8.0 software. The averages of intensities from six independent experiments were compared (for further information, see **Supplementary Table S1**). Analyzed proteins were then categorized into three groups: (A) increased (>2) proteins, (B) decreased (<0.5) proteins and (C) unchanged proteins (≥0.5 and ≤2). The numbers on the right side of the panels correspond to those shown in Fig 4.

be quantitatively determined because these high molecular weight or transmembrane proteins were not separated well on the 2D gels. We found that dynamin family proteins, DRP2A and DRP2B (#4), DRP1E (#8) and DRP1A (#9 and 10), and remorin family proteins (#35 and 36) accumulated in DRMs during the first 2 d of cold acclimation (**Fig. 5A**). In addition, proteins #24 and #25, neither of which could be identified, transiently increased >5-fold during cold acclimation. On the other hand, some of the V-ATPase peripheral V1 subunits, such as A (#7), B1 (#14), C (#23) and E (#34), rapidly decreased in DRMs during cold acclimation for 2 d (**Fig. 5B**). TUA and TUB (#16–19) and ACT2 and ACT8 (#22) decreased during cold acclimation. Patellin (#1) transiently decreased after 4 d of cold acclimation, but returned to the level in the non-acclimated sample thereafter. SKU5 (#5), Hsc70 (#6), PIRL4 (#11), TGG (#12 and 13), a nodulin-like protein (#15), eEF-1A (#20), an endomembrane-associated protein (#26), two remorin family proteins (#27–29) and three band 7 family proteins (#30–33) were not changed during cold acclimation for 7 d (**Fig. 5C**). Collectively, there were considerable changes in DRM proteins during the first 2 d of cold acclimation.

Western blot analysis of cold-responsive DRM proteins

Cold responses of DRM proteins were further confirmed using Western blot analysis with specific antibodies (**Fig. 6**). All proteins examined except for a cold-induced lipocalin-like protein (AtLCN; Kawamura and Uemura, 2003) were found in greater proportions in the DRM than in the PM. Clathrin heavy chain (CHC), a synaptotagmin homolog (SYT1) and aquaporin increased in DRM after cold acclimation, consistent with the results of SDS–PAGE in **Fig. 3**. P-ATPase temporarily increased after cold acclimation for 4 d. TUB decreased in DRMs during cold acclimation for 4 d and increased thereafter. Subunit E1 as well as subunit c (the same as spot #23 in **Table 4**) of V-ATPase decreased remarkably during the first 2 d of cold acclimation. There was a considerable decrease in actin just after cold acclimation for 2 d. The three members of band 7 family proteins (spots #30–33 in **Table 4**) exhibited very little change during cold acclimation for 2 d.

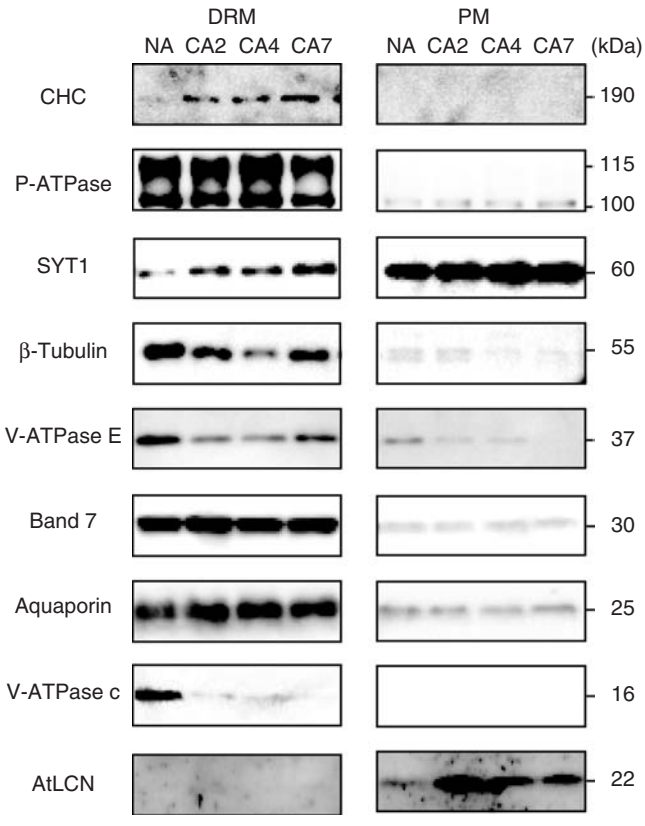

Fig. 6 Western blot analysis of cold-responsive DRM proteins. NA, non-acclimated; CA2, CA4 and CA7, cold acclimated for 2, 4 and 7 d, respectively. Proteins (1.5 μg) were visualized by horseradish peroxidase-conjugated goat anti-rabbit or anti-mouse IgG (H + L) antibodies after incubation with the antibody specific for the proteins indicated. Antibodies used were those for clathrin heavy chain (CHC), a synaptotagmin homolog (SYT1), P-ATPase, aquaporin, V-ATPase subunit c and E, β-tubulin and band 7 family protein. AtLCN, a lipocalin-like protein localized outside the DRM, was used as a reference.

Discussion

Cold acclimation effects on DRM compositions

Arabidopsis DRMs were recovered at 35–45% (w/w) sucrose concentrations after centrifugation. In animal cells, the DRM is typically collected at very low densities [i.e. 5/30% (w/v) of sucrose after centrifugation] (Brown and Rose 1992, Lisanti et al. 1994). However, plant DRMs have been reported to be collected at relatively high densities (Mongrand et al. 2004, Borner et al. 2005). There are considerable differences in the lipid-to-protein ratio of DRMs in animal and plant cells. The amount of total major lipids in DRMs of synaptic cells was >7 nmol μg^{-1} protein (Matsuura et al. 2007), while *Arabidopsis* DRM contained about 1.4 nmol μg^{-1} protein (**Table 1**). In the neutrophil PM, DRM fractions with higher densities were reported with many membrane skeleton proteins (Nebl et al. 2002). Thus, the lipid-to-protein ratio and the differences in lipid–protein association may affect the DRM density after centrifugation.

Cold acclimation resulted in various changes in DRM lipid composition (**Table 1** and **Fig. 1**), which may affect the number and size of microdomains. During cold acclimation, the amount of FS per protein increased and the DRM-to-PM ratios of ASG and SG became much greater. By using model membranes, plant sterols are able to promote lipid domain formation (Xu et al. 2001) and contribute temperature

Table 4 MALDI-TOF/MS and LC-MS/MS identification of DRM proteins in *Arabidopsis* separated by 2D-PAGE

No.	Exp. MM/pI (kDa/pI)[a]	Change[b]	Protein name[c]	Theo. MM/pI (D/pI)[d]	Accession No.	AGI code No.	TM[e]	MASCOT score[f]	MOWSE score[g]
1	97.1/4.5	↓	Patellin-1+	64,047/4.8	Q56WK6	At1g72150	0	211	1.94E + 21
			Patellin-2	76,008/4.6	Q56ZI2	At1g22530	0	103	–
2	98.2/5.0	ND	AtPLDδ (phospholipase Dδ)+	98,918/6.7	Q9C5Y0	At4g35790	0	–	3.69E + 11
3	104.5/6.5	ND	AHA1 (P-type H+-ATPase)	104,225/6.7	P20649	At2g18960	9	150	–
			TPR repeat-containing protein	90,170/6.7	O23052	At1g05150	0	159	–
4	103.6/10.1	↑	DRP2A (dynamin-related protein)	99,167/9.6	Q9SE83	At1g10290	0	231	–
			DRP2B (dynamin-related protein)	100,229/9.6	Q9LQ55	At1g59610	0	294	–
5	80.1/10.5	→	SKU5 (putative monocopper oxidase precursor)+	65,638/9.5	Q9SU40	At4g12420	1 (GPI)	–	5.78E + 17
6	71.4/4.8	→	Hsc70.1 (heat shock cognate 70 kDa protein 1)+	71,358/5.0	P22953	At5g02500	0	–	1.40E + 22
			or Hsc70.2+	71,387/4.8	P22954	At5g02490	0	–	1.40E + 22
			or Hsc70.3+	71,148/4.7	O65719	At3g09440	0	–	1.40E + 22
7	65.7/4.9	↓	VHA-A (V-type H+-ATPase subunit A)+	68,813/5.1	O23654	At1g78900	0	–	5.93E + 32
8	68.4/7.9	↑	DRP1E (dynamin-related protein)+	69,804/7.2	Q9FNX5	At3g60190	0	–	7.44E + 06
9, 10	65.8/9.5, 9.8	↑	DRP1A (dynamin-related protein)+	68,173/8.5	P42697	At5g42080	0	–	3.70E + 20, 9.80E + 20
11	60.8/5.3	→	PIRL4 (leucine-rich repeat protein)	60,996/5.3	Q9SVW8	At4g35470	0	182	–
12, 13	59.2/6.1, 6.3	→	Thioglucosidase (TGG2)	62,733/7.5	Q42595	At5g25980	1	204, 151	–
14	51.3/4.5	↓	VHA-B1 (V-type H+-ATPase subunit B) +	54,255/4.9	P11574	At1g76030	0	–	4.19E + 25
15	53.0/5.7	→	Nodulin-like protein (band 7 flotillin) +	52,310/5.9	Q501E6	At5g25250	0	359	1.20E + 11
			Nodulin-like protein (band 7 flotillin)	51,419/6.2	Q4V3D6	At5g25260	0	332	–
16	48.9/4.3	↓	TUB2 (tubulin β-2/β-3 chain)+	50,735/4.4	P29512	At5g62690/ At5g62700	0	–	2.19E + 30
			TUB6 (tubulin β-6 chain)+	50,586/4.4	P29514	At5g12250	0	–	3.05E + 29
			TUB7 (tubulin β-7 chain)+	50,747/4.5	P29515	At2g29550	0	–	2.70E + 29
17	48.0/4.3	↓	TUB4 (tubulin β-4 chain)+	49,824/4.5	P24636	At5g44340	0	–	2.19E + 30
			TUB9 (tubulin β-9 chain)+	49,659/4.4	P29517	At4g20890	0	–	4.18E + 24
			TUB5 (tubulin β-5 chain)+	50,343/4.4	P29513	At1g20010	0	–	2.19E + 24
18	48.9/4.6	↓	TUB4 (tubulin β-4 chain)+	49,824/4.5	P24636	At5g44340	0	–	6.71E + 19
19	48.0/4.6	↓	TUA6 (tubulin α-6 chain)+	49,538/4.7	P29511	At4g14960	0	–	4.35E + 18
			or TUA2 (tubulin α-2/α-4 chain)+	49,541/4.7	P29510	AAt1g04820/ At1g50010	0	–	4.35E + 18
20	48.8/10.5	→	eEF-1A (elongation factor 1-α) +	49,503/9.2	P13905	At1g07940/ At1g07920/ At1g07930/ At5g60390	0	–	1.96E + 19
21	42.6/10.0	ND	PIP2A (aquaporin)	30,474/8.6	P43286	At3g53420	5	99	–
22	43.2/4.9	↓	ACT8 (actin-8) +	41,863/5.3	Q96293	At1g49240	0	–	8.46E + 21
			or ACT2 (actin-2) +	41,877/5.3	Q96292	At3g18780	0	–	8.46E + 21
23	41.3/5.1	↓	VHA-C (V-type H+-ATPase subunit C)	42,620/5.2	Q9SDS7	At1g12840	0	418	–

continued

Table 4 Continued

No.	Exp. MM/pI (kDa/pI)[a]	Change[b]	Protein name[c]	Theo. MM/pI (D/pI)[d]	Accession No.	AGI code No.	TM[e]	MASCOT score[f]	MOWSE score[g]
24	36.0/6.1	↑	Not identified	–	–	–	–	–	–
25	37.6/8.2	↑	Not identified	–	–	–	–	–	–
26	37.5/4.6	→	Endomembrane-associated protein	24,569/5.0	Q2L6T2	At4g20260	0	172	–
27, 28	37.2/4.9, 5.1	→	Remorin family protein	23,144/5.3	Q9M2D8	At3g61260	0	269, 212	–
29	35.1/4.7	→	Remorin family protein	22,452/5.2	Q9FFA5	At5g23750	0	231	–
30	32.1/4.7	→	Band 7 family potein+	31,406/5.1	Q9CAR7	At1g69840	0	355	2.56E + 10
31	32.1/5.0	→	Band 7 family protein+	31,431/5.1	Q9FM19	At5g62740	0 (M)	132	1.69E + 07
32, 33	31.4/5.2, 5.6	→	Band 7 family protein+	31,321/5.5	Q9SRH6	At3g01290	0 (M)	261	5.75E + 29
34	31.4/6.0	↓	VHA-E (V-type H+-ATPase subunit E)	26,060/6.3	Q39258	At4g11150	0	297	–
35, 36	35.0/7.5, 8.5	↑	Remorin family protein	20,968/9.0	O80837	At2g45820	0	323, 252	–

Detailed information on changes in these proteins is shown in **Fig. 5** and **Supplementary Table S1**.

[a]Exp. MM/pI, experimentally obtained molecular mass and pI.

[b]Upward-pointing and downward-pointing arrows indicate increased (> 2) and decreased (< 0.5) spots during CA, respectively. Horizontal arrows indicate proteins with changes between 0.5- and 2-fold during CA. ND, not determined.

[c]A plus sign indicates proteins identified by MALDI-TOF/MS.

[d]Theo. MM/pI, theoretical molecular mass and pI determined from the database.

[e]TM, putative transmembrane domains predicted by SOSUI; GPI, glycosylphosphatidylinositol-anchored protein confirmed by Sedbrook et al. (2002); M, putative myristoylation site.

[f]MASCOT scores of proteins identified by LC-MS/MS are listed.

[g]MOWSE scores of proteins identified by MALDI-TOF/MS are listed.

dependence of membrane dynamics (Beck et al. 2007), suggesting that sterol lipids are deeply involved in the formation of membrane microdomains in plant cells during cold acclimation. GlcCer was enriched in DRMs, and its proportion did not alter much in DRMs after cold acclimation but decreased in the PM (**Table 1** and **Fig. 1**). Since GlcCer easily induces phase transition and forms domains (Norberg et al. 1996, Webb et al. 1997), changes in the distributional patterns of this lipid in the PM may affect membrane properties and microdomain formation. In addition, although there were only slight changes in the proportion of PLs in DRMs after cold acclimation, it is possible that changes in PLs in the PM affect microdomain formation. It has been reported that PLs in DRMs have more saturated fatty acids than do those in the PM (Mongrand et al. 2004), and addition of polyunsaturated fatty acid results in alterations in the size and distribution of microdomains (Chapkin et al. 2008). Furthermore, the composition of unsaturated fatty acids in the membrane/lipid raft was affected by growth temperature (Zehmer and Hazel 2005). Thus, it is possible that complex lipid changes in DRMs at the class and/or molecular species levels after cold acclimation collectively affect DRM formation and properties, which may result in a decrease in protein recovery in DRMs during cold acclimation (**Fig. 2**).

SDS–PAGE revealed clear differences in protein compositions in the total PM fractions and DRMs (**Fig. 3**). The number of proteins on the gel was clearly smaller in DRMs than in the PM fraction, and predominant proteins in DRMs were different from those in the total PM fraction. We previously identified cold-responsive proteins in the total PM fractions (Kawamura and Uemura 2003). Among a few hundred spots separated by 2D-PAGE, only 42 PM proteins were visibly altered during cold acclimation. On the other hand, in the present study, we revealed that many DRM proteins (20 to 40%) responded to cold (**Fig. 4D** and **Table 3**). These results indicated that the DRM contains a much greater proportion of cold-responsive proteins than does the total PM, suggesting active roles of the DRM in the cold acclimation process of plants.

It should be noted here that the 2D-PAGE-based analysis allowed us primarily to separate peripheral membrane proteins, including lipid-modified proteins, in DRMs and, hence, it may not be a suitable protocol for analysis of integral proteins. However, this protocol has been accepted for plant membrane proteome analysis. An *Arabidopsis* PM proteome analysis using nano-LC-MS/MS revealed that integral membrane proteins account for only 30% of the PM proteins (Alexandersson et al. 2004).

Proteomic analysis of DRM proteins and cold acclimation

In the present study, we identified 96 different proteins in the DRM using MS after separation by SDS–PAGE and 2D-PAGE, and classified them into categories, including

membrane transport (31 proteins), vesicle trafficking (14), cytoskeleton (14), microdomain-associated proteins (eight), PM and cell wall reconstruction-related proteins (eight), signal transduction (five) and others (18) (**Supplementary Table S2**). Furthermore, cold-responsive DRM proteins were found in the five categories: membrane transport, vesicle trafficking, cytoskeleton, microdomain-associated proteins and others (**Supplementary Table S1**). This is the first report showing that there is a dynamic change in the composition of DRM proteins in plant PM during cold acclimation.

H^+-ATPases and aquaporins, which are associated with membrane transport activity, increased in the DRM during cold acclimation (**Fig. 6**). H^+-ATPases function in ATP-dependent electrogenic proton movement across membranes and regulate cytoplasmic pH and membrane potential. P-ATPase activity is reported to increase in Jerusalem artichoke during cold acclimation (Ishikawa and Yoshida 1985). Yeast P-ATPase (Pma1p) is localized in DRMs, and the oligomerization of Pma1p occurs in membrane/lipid rafts (Bagnat et al. 2001, Lee et al. 2002). Thus, our finding suggests that cold treatment promotes the localization of P-ATPases into microdomains in the PM and may regulate P-ATPase activity during cold acclimation. Aquaporins have a key function in water transport across membranes (Preston et al. 1992). Cold treatment results in significant decreases in water uptake in the root system of freezing-tolerant plants (Fennell and Markhart 1998). Furthermore, at freezing temperatures, plant cells are severely dehydrated due to ice crystal growth in the extracellular region. Under these conditions, the water transport activity across the PM is an important factor for control of the amount of water in the cell (Levitt 1980). Overexpression of aquaporins in yeast increases osmotic water permeability at low temperatures (Soveral et al. 2006) and eventually increases freezing tolerance (Tanghe et al. 2002). Thus, it is possible that an increase in the proportion of aquaporins in plant DRMs improves osmotic water permeability of the PM at low and freezing temperatures and, hence, increases cell survival.

V-ATPase subunits were found in DRMs, and some of them decreased rapidly after cold acclimation for 1–2 d (**Table 4** and **Figs. 5**, **6**). Plant V-ATPases composed of a peripheral V1 domain and a transmembrane V0 domain (Dietz et al. 2001) are not only localized in the tonoplast (vacuolar membrane) but are also present in the PM and other endomembranes (Depta et al. 1991, Robinson et al. 1996, Kluge et al. 2004). V-ATPase activity is related to salt tolerance (Batelli et al. 2007) and is essential for the endocytotic membrane trafficking system through endosomal pH regulation (Stevens and Forgac 1997, Dettmer et al. 2006). Thus, it is possible that the V-ATPase in DRMs contributes to cold or freezing tolerance of *Arabidopsis* by way of regulation of membrane trafficking.

In addition, clathrin heavy chains and several dynamins, which are associated with the membrane vesicle trafficking system, were among cold-increased proteins in DRMs (**Table 4** and **Figs. 5**, **6**). Clathrin-mediated endocytosis is a system for removing extracellular substances and PM-localized receptors from the PM of mammalian cells (Roth 2006). Dynamins have been implicated in clathrin-coated vesicle budding from the PM (Battey et al. 1999, Hinshaw 2000). In *Arabidopsis*, dynamins have been reported to be involved in disease resistance, mitochondrial division, cell plate formation and fission of clathrin-coated vesicles in endocytosis (Hong et al. 2003, Tang et al. 2006). In particular, the DRP1 family is associated with the PM (Lam et al. 2002, Kang et al. 2003, Konopka et al. 2008), suggesting that these dynamins might function in the process of endocytosis in the plant PM. In addition, endocytosis that is visualized by staining with fluorescent dyes is strongly inhibited by cold treatment (Bolte et al. 2004). Taken together, our results suggest that accumulation of clathrin and dynamins in PM microdomains during cold acclimation may imply a delay of the clathrin-dependent endocytosis pathway in *Arabidopsis*.

It should be noted that because cold acclimation results in functional and compositional reconstitution of the PM (Steponkus et al. 1993) and some cold-responsive PM proteins are in fact regulated at the level of transcription at low temperatures (Tominaga et al. 2006, our unpublished results), the exocytosis pathway must be active to transport lipid and protein components from the endoplasmic reticulum to the PM during cold acclimation. Our data revealed that a putative exocytosis-related protein, SYT1, which has recently been reported to be associated with the membrane fusion event (Yamazaki et al. 2009), increased in the DRM as well as in the PM during cold acclimation (**Fig. 6**). These findings suggest that cold-induced reconstitution of the PM is mediated by cold-specific membrane trafficking systems, which are different from those occurring at normal temperatures.

Cold acclimation results in decreases in cytoskeleton-associated proteins in the DRM, such as tubulins (TUA and TUB) and actins (ACT8 or ACT2) (**Table 4** and **Figs. 5, 6**). Microtubules consist of TUA and TUB heterodimers and play an important role in the development of freezing tolerance. In winter rye, microtubules depolymerize more readily in cold-acclimated root cells under freezing temperatures than in non-acclimated root cells, which is closely associated with the extent of freezing tolerance (Kerr and Carter 1990). In several wheat cultivars, microtubule disassembly during cold acclimation is correlated with the extent of development of freezing tolerance and associated with decreases in the total amount of TUA (Abdrakhamanova et al. 2003). Furthermore, in animal cells, microtubules and actin filaments are in many cases associated with membrane/lipid rafts and regulate the movement and localization of proteins in

microdomains (Head et al. 2006). Cold treatment results in depolymerization of actin filaments in tobacco cells (Pokorna et al. 2004). Orvar et al. (2000) interestingly demonstrated that membrane rigidification induces disruption of actin filaments and that the disruption triggers a signal transduction for cold acclimation in alfalfa. These results collectively suggest that PM microdomains are the site for PM–cytoskeleton interactions mediated through cytoskeleton-associated proteins in the DRM and that freezing stress or low temperature sensing events results in changes in the cytoskeleton assembly at the PM microdomains.

Conclusions and future perspectives

We demonstrated that lipid and protein compositions of the DRM in the *Arabidopsis* PM change both qualitatively and quantitatively during cold acclimation. The lipid composition of the DRM, which is enriched in sterols and GlcCer and is considerably different from that of the total PM fraction, responded to cold such that there was an increase in FS with a corresponding decrease in PLs. Because the DRM in general is the place for the important physiological reactions such as membrane transport, intracellular vesicle trafficking and cytoskeleton connections, cold-induced alterations in the lipid composition of the DRM may result in modification of the function mediated by DRM proteins. In fact, P-ATPase activity is regulated by membrane environmental factors such as membrane lipids (Kasamo 2003). Furthermore, it is suggested that lipid components can regulate the protein targeting process so that the protein composition of the DRM becomes vastly different from that in the total PM (Borner et al. 2005). The effect of the lipid environment on protein activity and targeting has been also reported in animal cells (Rodal et al. 1999, Cornelius 2001, Pike 2005, Schley et al. 2006). Thus, it is possible that cold acclimation induces lipid changes in the DRM and the PM, which affects protein populations and activities in the DRM and, hence, modifies the survival ability of the cells under low temperatures.

Changes in DRM proteins during cold acclimation can be explained by three events: transcriptional regulation, modification of distributional patterns within the PM and/or accumulation due to repressed membrane trafficking. Interestingly, real-time PCR experiments revealed that there was no relationship between changes in the majority of cold-responsive proteins in the DRM and their transcription levels (Minami et al. 2008). It is likely that lipid changes in the DRM as well as in the PM affect protein distribution in the DRM and PM. Furthermore, the rate or the extent of membrane trafficking events will be considerably influenced by cold acclimation, which may result in accumulation of proteins associated with these events in the DRM. Thus, changes in DRM proteins during cold acclimation may be primarily due to the modification of distributional patterns of proteins within the PM and/or accumulation due to repressed membrane trafficking. Nevertheless, it is necessary to elucidate and understand further the molecular mechanism of protein changes in the DRM during cold acclimation. This information is a prerequisite for us to examine the role of each cold-responsive DRM protein in the plant cold acclimation process.

Materials and Methods

Plant materials

Seeds of *A. thaliana* L. Heyn (ecotype Columbia) were planted and grown under continuous light conditions at 50 µmol m^{-2} s^{-1} at soil level as described previously (Uemura et al. 1995). Three- to 4-week-old seedlings before bolting were used as non-acclimated plants. Cold-acclimated plants were obtained by transferring non-acclimated plants to a controlled environment chamber at 2°C (8 h photoperiod at 75 mol m^{-2} s^{-1} at soil level) for 2–7 d.

Isolation of PM fractions and DRMs

Non-acclimated or cold-acclimated seedlings were excised and immediately used for preparation of PM fractions using a polyethylene glycol–dextran aqueous two-phase partition system (Uemura et al. 1995). The two-phase partition was repeated three times to increase the purity of the PM. Protein content in the PM fractions was determined by the Bradford assay (Bio-Rad, Munich, Germany) using bovine serum albumin (BSA) as a standard.

DRMs were isolated from the PM fractions according to the method of Peskan et al. (2000). An aliquot of the PM fractions (2 mg protein equivalent) was suspended in 2.7 ml of TED buffer [50 mM Tris–HCl (pH 7.4), 3 mM EDTA and 1 mM dithiothreitol (DTT)]. After addition of 300 µl of 10% (w/v) Triton X-100 [at a final ratio of 15 : 1, Triton X-100/protein (w/w)], the PM–Triton X-100 solution was incubated for 30 min on ice. The sample was then mixed with 12 ml of 65% (w/w) sucrose in TED buffer [final sucrose concentration, 52% (w/w)], placed at the bottom of a centrifuge tube and overlaid with sucrose solutions at concentrations of 35, 30 and 5% (w/w) successively. The gradients were then centrifuged at 141,000×g(R_{max}) in a P28S rotor (Hitachi, Tokyo, Japan) for 20 h at 4°C. The DRMs at 35–45% (w/v) sucrose were collected, diluted with TED buffer and then pelleted at 231,000×g(R_{max}) for 35 min at 4°C in an RT50 rotor (Hitachi). Protein content in the DRM was determined as described above.

Lipid analysis

Lipids were extracted from PM fractions and DRMs according to the method of Bligh and Dyer (1959). Total lipid extracts were separated by TLC (Silica gel 60, 0.25 mm in thickness, Merck, Darmstadt, Germany) with a solvent mixture of

chloroform, methanol and water (65:25:4, by vol.). Individual lipids were identified by co-chromatography with authentic standard lipids. Separated lipids were detected under UV light after spraying of primuline [0.1% (w/v) in 80% (v/v) acetone]. Quantification of each lipid was performed according to the method of Uemura et al. (1995).

Gel electrophoresis

For SDS–PAGE analysis, protein samples were resuspended in SDS sample buffer [2% (w/v) SDS, 50 mM Tris–HCl (pH 6.8), 6% (v/v) β-mercaptoethanol, 10% (w/v) glycerol and bromophenol blue]. After being separated by 10% SDS–PAGE, proteins were visualized by the silver staining method (Kawamura and Uemura 2003).

For 2D-PAGE analysis, DRM samples (50 μg of proteins) were pre-purified using a 2D-Clean-up kit (GE Healthcare, Little Chalfont, Buckinghamshire, UK) and then subjected to isoelectrofocusing electrophoresis using an immobilized linear pH gradient-forming gel strip (GE Healthcare, Immobiline™ DryStrip pH 3–11 NL, 11 cm). Strips were rehydrated at 20°C for 12 h at 100 V with protein solutions containing 7 M urea, 2 M thiourea, 2% (w/v) ABS-14, 0.5% (w/v) Triton X-100, 1.2% (v/v) DeStreak Reagent (GE Healthcare) and 0.5% (v/v) IpG buffer (GE Healthcare), and isoelectrofocused at 20°C on an IPGphor system (GE Healthcare) with a successive increase in voltage [500 V (1 h), 1,000 V (1 h), 2,000 V (1 h), 4,000 V (1 h), 6,000 V (2 h) and 8,000 V (4 h)]. Gel strips were then equilibrated in a denaturing solution [6 M urea, 1% (w/v) DTT, 30% (w/v) glycerol, 4% (w/v) SDS, 50 mM Tris–HCl (pH 6.8) and bromophenol blue] and subsequently subjected to 10% SDS–PAGE as described above. Proteins were visualized by silver staining.

2D-DIGE

Aliquots of DRMs (50 μg of proteins) were purified using the 2D-Clean-up kit and then resuspended in a lysis buffer [7 M urea, 2 M thiourea, 2% (w/v) ABS-14, 0.5% (w/v) Triton X-100 and 10 mM Tris–HCl (pH 8.5)]. 2D-DIGE analyses were carried out according to the manufacturer's CyDye DIGE Fluors protocol (minimal dyes, GE Healthcare). Each protein sample (20 μg of proteins) was minimally labeled with Cy3 or Cy5 dye. As an internal standard, equal amounts of proteins of all samples to be analyzed were mixed and labeled with Cy2. The labeling reaction was performed by incubating the samples on ice for 30 min in the dark, quenched by addition of 1 μl of 10 mM lysine, and mixed with an equal volume of 2× sample buffer [7 M urea, 2 M thiourea, 2% (w/v) ABS-14, 0.5% (w/v) Triton X-100, 1.2% DeStreak Reagent and 2% (v/v) IpG buffer]. Two 2D-DIGE gels were used as a set for differential expression analysis of DRM proteins during cold acclimation. For the first gel, the three differentially labeled samples, non-acclimation (Cy3 or Cy5), cold acclimation for 4 d (Cy5 or Cy3) and the internal standard (Cy2), were mixed. For the second gel, the three samples, cold acclimation for 2 d (Cy3 or Cy5), cold acclimation for 7 d (Cy5 or Cy3) and the internal standard (Cy2), were mixed. After adjusting the volume to 350 μl with rehydration buffer [2× sample buffer except for the concentration of IpG buffer being 0.5% (v/v)], the samples were loaded onto isoelectrofocusing gel strips with an immobilized linear pH gradient (Immobiline™ DryStrip pH 3–11 NL, 18 cm). The strips were rehydrated at 20°C for 12 h at 100 V with the protein samples and then isoelectrofocused at 20°C in the IPGphor system with a successive increase in voltage [500 V (1 h), 1,000 V (1 h), 2,000 V (1 h), 4,000 V (1 h), 5,000 V (1 h), 6,000 V (2 h) and 8,000 V (7 h)]. Gel strips were subjected to 10% SDS–PAGE as described above.

After electrophoresis, three CyDye images from one gel were visualized using a Molecular Imager FX (Bio-Rad) in fluorescence mode with a pixel size of 100 μm. The Cy2, Cy3 and Cy5 fluorescence was imaged using excitation/emission wavelengths of 488/530, 532/605 and 635/695 nm, respectively. Typically, three biologically independent samples of DRMs in each of non-acclimated and 2, 4 and 7 d cold-acclimated seedlings were prepared, and two technical replications in each biological sample were performed. Thus, a total of 36 gel images (containing 12 internal standard images) were obtained in the experiments, and the captured gel images were analyzed using PDQuest V 8.0 software (Bio-Rad). The intensities of protein spots from the Cy3 and Cy5 images were normalized using the Cy2-labeled internal standard in a local regression model. For Student's *t*-test analysis, the fluorescent intensity of each protein spot was normalized to that of the Cy2-labeled internal standard and then compared with the averaged value of the non-acclimated sample.

MALDI-TOF/MS and LC-MS/MS

Protein bands or spots after electrophoresis were cut out from gels after being visualized. Peptide mass fingerprinting analysis combined with MALDI-TOF/MS was performed as described previously (Kawamura and Uemura 2003). Peptide mass fingerprint data from five independent samples were matched to the MS-Fit program of the protein prospector package (http://prospector.ucsf.edu/).

For LC-MS/MS, trypsin-digested peptides were prepared by the same method as that used for the MALDI-TOF/MS analysis. Quadrupole Time-of-Flight (Q-TOF). LC-MS/MS analysis was performed as described previously with a Waters CapLC system and a Q-TOF mass spectrometer (Waters, Milford, MA, USA) (Fujiwara et al. 2006). In some cases, LC-MS/MS analysis was performed with an HCTultra ESI-ion-trap mass spectrometer (Bruker Daltonics, Leipzig, Germany) equipped with an Agilent 1100 CapLC system (Agilent, Wilmington, DE, USA). The digested peptides were loaded into a reversed-phase column (Zorbax 300S-C18,

3.5 µm, 150×0.3 mm, Agilent) in a CapLC, eluted in a linear gradient from 10 to 65% (v/v) of acetonitrile in 0.1% (w/w) formic acid over a period of 30 min at a flow rate of 4 µl min^{-1} after a hold at 10% (v/v) of acetonitrile for 5 min, and introduced into a mass spectrometer. A mass spectrum with a range of 200 and 1,800 *m/z* was acquired using the Esquire Control program (version 6.1). MS/MS spectra were searched against the protein database of the National Center for Biotechnology Information using the MASCOT MS/MS ion search server (Matrix Science, http://www.matrixscience.com). The searches were performed with the following parameters: allowed one missed cleavage, fixed modifications for carbamidomethyl (C), variable modifications for phospho (ST/Y) and oxidation (M), peptide tolerance of ±0.5 Da, MS/MS tolerance of ±0.3 Da, and peptide charge of 1 +, 2 + and 3 +; and instrument, ESI-TRAP.

Western blot analysis

Samples (1.5 µg of proteins each) were separated by 15 or 10% SDS–PAGE and electrotransferred onto polyvinylidene fluoride membranes using a horizontal semi-dry Western blotter. The membranes were then blocked with 5% (w/v) skim milk in phosphate-buffered saline (PBS) and immunoblotted with the following antibodies: clathrin heavy chain 4A8 (1:1,000 dilution; Abcam, http://www.abcam.com/), P-ATPase (1:14,000 dilution; Morsomme et al. 1998), aquaporin (1:4,000 dilution; Ohshima et al. 2001), V-ATPase subunits c and E (1:2,000 dilution; Kawamura et al. 2000), β-tubulin Tub2.1 (1:500 dilution; Sigma-Aldrich, St Louis, MO, USA), AtLCN, which is a lipocalin-like protein (1:2,000 dilution, Tominaga et al. unpublished) and SYT1 (1:2,000 dilution, Yamazaki et al. 2009). Polyclonal antibody against band 7 family proteins was prepared in our laboratory. Briefly, the full-length At1g69840 coding sequence was cloned into pENTR/D-TOPO, transferred into the pDEST-17 vector (Invitrogen, Carlsbad, CA, USA), and expressed in *Escherichia coli* strain BL21 (DE3) as a His tag-conjugated band 7 family protein. A rabbit polyclonal antibody against purified His tag-conjugated band 7 family protein was prepared by T. K. Craft (Japan) and used at a 1:2,000 dilution. After incubation with horseradish peroxidase-conjugated goat anti-rabbit or anti-mouse IgG (H + L) secondary antibodies (1:2,000 dilution; Pierce, Rockford, IL, USA), signals were detected using Super-Signal West Femto Maximum Sensitivity Substrate (Pierce) in a LightCapture system (ATTO, Tokyo, Japan).

Supplementary data

Supplementary data are available at PCP online.

Funding

The Ministry of Education, Culture, Sports, Science and Technology of Japan Grant-in-Aids for Scientific Research (No. 18880005 to A.M., No. 17380062 to M.U.); the 21st Century Center of Excellence Program (No. K-3 to M.U.); the High-Tech Research Project (2005–2009 to M.K.).

Acknowledgments

We are indebted the following people for their kind gifts of antibodies used in the study: Drs. Marc Boutry and Toshinori Kinoshita for P-ATPase, Drs. Masayoshi Maeshima and Junko Sakurai for aquaporin, and Dr. Yoko Tominaga for lipocalin. We also thank Professor Michael Schlappi for critical reading of the manuscript.

References

Abdrakhamanova, A., Wang, Q.Y., Khokhlova, L. and Nick, P. (2003) Is microtubule disassembly a trigger for cold acclimation? *Plant Cell Physiol.* 44: 676–686.

Alexandersson, E., Saalbach, G., Larsson, C. and Kjellbom, P. (2004) *Arabidopsis* plasma membrane proteomics identifies components of transport, signal transduction and membrane trafficking. *Plant Cell Physiol.* 45: 1543–1556.

Anderson, R.G. and Jacobson, K. (2002) A role for lipid shells in targeting proteins to caveolae, rafts, and other lipid domains. *Science* 296: 1821–1825.

Bagnat, M., Chang, A. and Simons, K. (2001) Plasma membrane proton ATPase Pma1p requires raft association for surface delivery in yeast. *Mol. Biol. Cell* 12: 4129–4138.

Batelli, G., Verslues, P.E., Agius, F., Qiu, Q., Fujii, H., Pan, S., et al. (2007) SOS2 promotes salt tolerance in part by interacting with the vacuolar H^+-ATPase and upregulating its transport activity. *Mol. Cell Biol.* 27: 7781–7790.

Battey, N.H., James, N.C., Greenland, A.J. and Brownlee, C. (1999) Exocytosis and endocytosis. *Plant Cell* 11: 643–660.

Beck, J.G., Mathieu, D., Loudet, C., Buchoux, S. and Dufourc, E.J. (2007) Plant sterols in 'rafts': a better way to regulate membrane thermal shocks. *FASEB J.* 21: 1714–1723.

Berczi, A. and Horvath, G. (2003) Lipid rafts in the plant plasma membrane? *Acta Biol. Szeged* 47: 7–10.

Bhat, R.A., Miklis, M., Schmelzer, E., Schulze-Lefert, P. and Panstruga, R. (2005) Recruitment and interaction dynamics of plant penetration resistance components in a plasma membrane microdomain. *Proc. Natl Acad. Sci. USA* 102: 3135–3140.

Bhat, R.A. and Panstruga, R. (2005) Lipid rafts in plants. *Planta* 223: 5–19.

Bligh, E.G. and Dyer, W.J. (1959) A rapid method of total lipid extraction and purification. *Can. J. Bot.* 37: 911–917.

Bloch, D., Lavy, M., Efrat, Y., Efroni, I., Bracha-Drori, K., Abu-Abied, M., et al. (2005) Ectopic expression of an activated RAC in *Arabidopsis* disrupts membrane cycling. *Mol. Biol. Cell* 16: 1913–1927.

Bolte, S., Talbot, C., Boutte, Y., Catrice, O., Read, N.D. and Satiat-Jeunemaitre, B. (2004) FM-dyes as experimental probes for dissecting vesicle trafficking in living plant cells. *J. Microsc.* 214: 159–173.

Borner, G.H., Sherrier, D.J., Weimar, T., Michaelson, L.V., Hawkins, N.D., Macaskill, A., et al. (2005) Analysis of detergent-resistant membranes in *Arabidopsis*: evidence for plasma membrane lipid rafts. *Plant Physiol.* 137: 104–116.

Brown, D.A. and Rose, J.K. (1992) Sorting of GPI-anchored proteins to glycolipid-enriched membrane subdomains during transport to the apical cell surface. *Cell* 68: 533–544.

Brown, D.A. and London, E. (1998) Structure and origin of ordered lipid domains in biological membranes. *J. Membr. Biol.* 164: 103–114.

Bunai, K. and Yamane, K. (2005) Effectiveness and limitation of two-dimensional gel electrophoresis in bacterial membrane protein proteomics and perspectives. *J. Chromatogr. B* 5: 227–236.

Cahoon, E.B. and Lynch, D.V. (1991) Analysis of glucocerebrosides of rye (*Secale cereale* L. cv Puma) leaf and plasma membrane. *Plant Physiol.* 95: 58–68.

Chapkin, R.S., Wang, N., Fan, Y.Y., Lupton, J.R. and Prior, I.A. (2008) Docosahexaenoic acid alters the size and distribution of cell surface microdomains. *Biochim. Biophys. Acta* 1778: 466–471.

Cornelius, F. (2001) Modulation of Na,K-ATPase and Na-ATPase activity by phospholipids and cholesterol. I. Steady-state kinetics. *Biochemistry* 40: 8842–8851.

Depta, H., Holstein, S.E.H., Robinson, D.G., Luetzelschwab, M. and Michalke, W. (1991) Membrane markers in highly purified clathrin-coated vesicles from *Cucurbita* hypocotyls. *Planta* 183: 434–442.

Dettmer, J., Hong-Hermesdorf, A., Stierhof, Y.D. and Schumacher, K. (2006) Vacuolar H^+-ATPase activity is required for endocytic and secretory trafficking in *Arabidopsis*. *Plant Cell* 18: 715–730.

Dietz, K.J., Tavakoli, N., Kluge, C., Mimura, T., Sharma, S.S., Harris, G.C., et al. (2001) Significance of the V-type ATPase for the adaptation to stressful growth conditions and its regulation on the molecular and biochemical level. *J. Exp. Bot.* 52: 1969–1980.

Fennell, A. and Markhart, A.H. (1998) Rapid acclimation of root hydraulic conductivity to low temperature. *J. Exp. Bot.* 49: 879–884.

Fujiwara, M., Umemura, K., Kawasaki, T. and Shimamoto, K. (2006) Proteomics of Rac GTPase signaling reveals its predominant role in elicitor-induced defense response of cultured rice cells. *Plant Physiol.* 140: 734–745.

Gilmour, S.J. and Thomashow, M.F. (1991) Cold acclimation and cold-regulated gene expression in ABA mutants of *Arabidopsis thaliana*. *Plant Mol. Biol.* 17: 1233–1240.

Guy, C.L. (1990) Cold acclimation and freezing stress tolerance: role of protein metabolism. *Annu. Rev. Plant Physiol. Plant Mol. Biol.* 41: 187–223.

Head, B.P., Patel, H.H., Roth, D.M., Murray, F., Swaney, J.S., Niesman, I.R., et al. (2006) Microtubules and actin microfilaments regulate lipid raft/caveolae localization of adenylyl cyclase signaling components. *J. Biol. Chem.* 281: 26391–26399.

Hinshaw, J.E. (2000) Dynamin and its role in membrane fission. *Annu. Rev. Cell Dev. Biol.* 16: 483–519.

Hong, Z., Geisler-Lee, C.J., Zhang, Z. and Verma, D.P. (2003) Phragmoplastin dynamics: multiple forms, microtubule association and their roles in cell plate formation in plants. *Plant Mol. Biol.* 53: 297–312.

Ishikawa, M. and Yoshida, S. (1985) Seasonal changes in plasma membranes and mitochondria isolated from Jerusalem artichoke tubers: possible relationship to cold hardiness. *Plant Cell Physiol.* 90: 1088–1095.

Kang, B.H., Busse, J.S. and Bednarek, S.Y. (2003) Members of the *Arabidopsis* dynamin-like gene family, *ADL1*, are essential for plant cytokinesis and polarized cell growth. *Plant Cell* 15: 899–913.

Kasamo, K. (2003) Regulation of plasma membrane H^+-ATPase activity by the membrane environment. *J. Plant Res.* 116: 517–523.

Kawamura, Y., Arakawa, K., Maeshima, M. and Yoshida, S. (2000) Tissue specificity of E subunit isoforms of plant vacuolar H^+-ATPase and existence of isotype enzymes. *J. Biol. Chem.* 275: 6515–6522.

Kawamura, Y. and Uemura, M. (2003) Mass spectrometric approach for identifying putative plasma membrane proteins of *Arabidopsis* leaves associated with cold acclimation. *Plant J.* 36: 141–154.

Kerr, G.P. and Carter, J.V. (1990) Relationship between freezing tolerance of root-tip cells and cold stability of microtubules in rye (*Secale cereale* L. cv Puma). *Plant Physiol.* 93: 77–82.

Kluge, C., Seidel, T., Bolte, S., Sharma, S.S., Hanitzsch, M., Satiat-Jeunemaitre, B., et al. (2004) Subcellular distribution of the V-ATPase complex in plant cells, and in vivo localisation of the 100 kDa subunit VHA-a within the complex. *BMC Cell Biol.* 5: 29.

Konopka, C.A., Backues, S.K. and Bednarek, S.Y. (2008) Dynamics of *Arabidopsis* dynamin-related protein 1C and a clathrin light chain at the plasma membrane. *Plant Cell* 20: 1363–1380.

Kusumi, A., Nakada, C., Ritchie, K., Murase, K., Suzuki, K., Murakoshi, H., et al. (2005) Paradigm shift of the plasma membrane concept from the two-dimensional continuum fluid to the partitioned fluid: high-speed single-molecule tracking of membrane molecules. *Annu. Rev. Biophys. Biomol. Struct.* 34: 351–378.

Laloi, M., Perret, A.M., Chatre, L., Melser, S., Cantrel, C., Vaultier, M.N., et al. (2007) Insights into the role of specific lipids in the formation and delivery of lipid microdomains to the plasma membrane of plant cells. *Plant Physiol.* 143: 461–472.

Lam, B.C., Sage, T.L., Bianchi, F. and Blumwald, E. (2002) Regulation of ADL6 activity by its associated molecular network. *Plant J.* 31: 565–576.

Langhorst, M.F., Reuter, A. and Stuermer, C.A. (2005) Scaffolding microdomains and beyond: the function of reggie/flotillin proteins. *Cell Mol. Life Sci.* 62: 2228–2240.

Lee, M.C., Hamamoto, S. and Schekman, R. (2002) Ceramide biosynthesis is required for the formation of the oligomeric H^+-ATPase Pma1p in the yeast endoplasmic reticulum. *J. Biol. Chem.* 277: 22395–22401.

Lefebvre, B., Furt, F., Hartmann, M.A., Michaelson, L.V., Carde, J.P., Sargueil-Boiron, F., et al. (2007) Characterization of lipid rafts from *Medicago truncatula* root plasma membranes: a proteomic study reveals the presence of a raft-associated redox system. *Plant Physiol.* 144: 402–418.

Levitt, J. (1980) Responses of Plants to Environmental Stresses, 2nd edn. Academic Press, New York.

Li, W., Li, M., Zhang, W., Welti, R. and Wang, X. (2004) The plasma membrane-bound phospholipase Dδ enhances freezing tolerance in *Arabidopsis thaliana*. *Nat. Biotechnol.* 22: 427–433.

Lillemeier, B.F., Pfeiffer, J.R., Surviladze, Z., Wilson, B.S. and Davis, M.M. (2006) Plasma membrane-associated proteins are clustered into islands attached to the cytoskeleton. *Proc. Natl Acad. Sci. USA* 103: 18992–18997.

Lisanti, M.P., Scherer, P.E., Vidugiriene, J., Tang, Z., Hermanowski-Vosatka, A., Tu, Y.H., et al. (1994) Characterization of caveolin-rich membrane domains isolated from an endothelial-rich source: implications for human disease. *J. Cell Biol.* 126: 111–126.

Lynch, D.V. and Steponkus, P.L. (1987) Plasma membrane lipid alterations associated with cold acclimation of winter rye seedlings (*Secale cereale* L. cv Puma). *Plant Physiol.* 83: 761–767.

Marouga, R., David, S. and Hawkins, E. (2005) The development of the DIGE system: 2D fluorescence difference gel analysis technology. *Anal. Bioanal. Chem.* 382: 669–678.

Matsuura, D., Taguchi, K., Yagisawa, H. and Maekawa, S. (2007) Lipid components in the detergent-resistant membrane microdomain (DRM) obtained from the synaptic plasma membrane of rat brain. *Neurosci. Lett.* 423: 158–161.

Mazars, C., Thion, L., Thuleau, P., Graziana, A., Knight, M.R., Moreau, M., et al. (1997) Organization of cytoskeleton controls the changes in cytosolic calcium of cold-shocked *Nicotiana plumbaginifolia* protoplasts. *Cell Calcium* 22: 413–420.

Minami, A., Furuto, A. and Uemura, M. (2008) Cold response of plant microdomain-associated proteins. *Cryobiol. Cryotechnol.* 54 (in press, in Japanese with English summary).

Mongrand, S., Morel, J., Laroche, J., Claverol, S., Carde, J.P., Hartmann, M.A., et al. (2004) Lipid rafts in higher plant cells: purification and characterization of Triton X-100-insoluble microdomains from tobacco plasma membrane. *J. Biol. Chem.* 279: 36277–36286.

Morel, J., Claverol, S., Mongrand, S., Furt, F., Fromentin, J., Bessoule, J.J., et al. (2006) Proteomics of plant detergent-resistant membranes. *Mol. Cell Proteomics* 5: 1396–1411.

Morsomme, P., Dambly, S., Maudoux, O. and Boutry, M. (1998) Single point mutations distributed in 10 soluble and membrane regions of the *Nicotiana plumbaginifolia* plasma membrane PMA2 H^+-ATPase activate the enzyme and modify the structure of the C-terminal region. *J. Biol. Chem.* 273: 34837–34842.

Nadimpalli, R., Yalpani, N., Johal, G.S. and Simmons, C.R. (2000) Prohibitins, stomatins, and plant disease response genes compose a protein superfamily that controls cell proliferation, ion channel regulation, and death. *J. Biol. Chem.* 275: 29579–29586.

Nebl, T., Pestonjamasp, K.N., Leszyk, J.D., Crowley, J.L., Oh, S.W. and Luna, E.J. (2002) Proteomic analysis of a detergent-resistant membrane skeleton from neutrophil plasma membranes. *J. Biol. Chem.* 277: 43399–43409.

Norberg, P., Nilsson, R., Nyiredy, S. and Liljenberg, C. (1996) Glucosylceramides of oat root plasma membranes—physicochemical behaviour in natural and in model systems. *Biochim. Biophys. Acta* 1299: 80–86.

Ohshima, Y., Iwasaki, I., Suga, S., Murakami, M., Inoue, K. and Maeshima, M. (2001) Low aquaporin content and low osmotic water permeability of the plasma and vacuolar membranes of a CAM plant *Graptopetalum paraguayense*: comparison with radish. *Plant Cell Physiol.* 42: 1119–1129.

Orvar, B.L., Sangwan, V., Omann, F. and Dhindsa, R.S. (2000) Early steps in cold sensing by plant cells: the role of actin cytoskeleton and membrane fluidity. *Plant J.* 23: 785–794.

Peskan, T., Westermann, M. and Oelmuller, R. (2000) Identification of low-density Triton X-100-insoluble plasma membrane microdomains in higher plants. *Eur. J. Biochem.* 267: 6989–6995.

Peterman, T.K., Ohol, Y.M., McReynolds, L.J. and Luna, E.J. (2004) Patellin1, a novel Sec14-like protein, localizes to the cell plate and binds phosphoinositides. *Plant Physiol.* 136: 3080–3094.

Pike, L.J. (2005) Growth factor receptors, lipid rafts and caveolae: an evolving story. *Biochim. Biophys. Acta* 1746: 260–273.

Pokorna, J., Schwarzerova, K., Zelenkova, S., Petrasek, J., Janotova, I., Capkova, V., et al. (2004) Sites of actin filament initiation and reorganization in cold-treated tobacco cells. *Plant Cell Environ.* 27: 641–653.

Preston, G.M., Carroll, T.P., Guggino, W.B. and Agre, P. (1992) Appearance of water channels in Xenopus oocytes expressing red cell CHIP28 protein. *Science* 256: 385–387.

Rajendran, L. and Simons, K. (2005) Lipid rafts and membrane dynamics. *J. Cell Sci.* 118: 1099–1102.

Robinson, D.G., Haschke, H.-P., Hinz, G., Hoh, B., Maeshima, M. and Marty, F. (1996) Immunological detection of tonoplast polypeptides in the plasma membrane of pea cotyledons. *Planta* 198: 95–103.

Rodal, S.K., Skretting, G., Garred, O., Vilhardt, F., van Deurs, B. and Sandvig, K. (1999) Extraction of cholesterol with methyl-beta-cyclodextrin perturbs formation of clathrin-coated endocytic vesicles. *Mol. Biol. Cell* 10: 961–974.

Roth, M.G. (2006) Clathrin-mediated endocytosis before fluorescent proteins. *Nat. Rev. Mol. Cell Biol.* 7: 63–68.

Salzer, U. and Prohaska, R. (2001) Stomatin, flotillin-1, and flotillin-2 are major integral proteins of erythrocyte lipid rafts. *Blood* 97: 1141–1143.

Sangwan, V., Foulds, I., Singh, J. and Dhindsa, R.S. (2001) Cold-activation of *Brassica napus BN115* promoter is mediated by structural changes in membranes and cytoskeleton, and requires Ca^{2+} influx. *Plant J.* 27: 1–12.

Schley, P.D., Brindley, D.N. and Field, C.J. (2007) (n-3) PUFA alter raft lipid composition and decrease epidermal growth factor receptor levels in lipid rafts of human breast cancer cells. *J. Nutr.* 137: 548–553.

Schroeder, R., London, E. and Brown, D. (1994) Interactions between saturated acyl chains confer detergent resistance on lipids and glycosylphosphatidylinositol (GPI)-anchored proteins: GPI-anchored proteins in liposomes and cells show similar behavior. *Proc. Natl Acad. Sci. USA* 91: 12130–12134.

Sedbrook, J.C., Carroll, K.L., Hung, K.F., Masson, P.H. and Somerville, C.R. (2002) The *Arabidopsis SKU5* gene encodes an extracellular glycosyl phosphatidylinositol-anchored glycoprotein involved in directional root growth. *Plant Cell* 14: 1635–1648.

Shahollari, B., Peskan-Berghofer, T. and Oelmuller, R. (2004) Receptor kinases with leucine-rich repeats are enriched in Triton X-100 insoluble plasma membrane microdomains from plants. *Physiol. Plant.* 122: 394–403.

Shahollari, B., Vadassery, J., Varma, A. and Oelmuller, R. (2007) A leucine-rich repeat protein is required for growth promotion and enhanced seed production mediated by the endophytic fungus *Piriformospora indica* in *Arabidopsis thaliana*. *Plant J.* 50: 1–13.

Sharma, P., Sharma, N. and Deswal, R. (2005) The molecular biology of the low-temperature response in plants. *BioEssays* 27: 1048–1059.

Simons, K. and Ikonen, E. (1997) Functional rafts in cell membranes. *Nature* 387: 569–572.

Simons, K. and Toomre, D. (2000) Lipid rafts and signal transduction. *Nat. Rev. Mol. Cell Biol.* 1: 31–39.

Soveral, G., Veiga, A., Loureiro-Dias, M.C., Tanghe, A., Van Dijck, P. and Moura, T.F. (2006) Water channels are important for osmotic adjustments of yeast cells at low temperature. *Microbiology*, 152: 1515–1521.

Steponkus, P.L., Uemura, M. and Webb, M.S. (1993) A contrast of the cryostability of the plasma membrane of winter rye and spring oat—two species that widely differ in their freezing tolerance and plasma membrane lipid composition. *In* Advances in Low Temperature Biology. Edited by Steponkus, P.L. Vol. 2, pp. 211–312. JAI Press, London.

Stevens, T.H. and Forgac, M. (1997) Structure, function and regulation of the vacuolar H^+-ATPase. *Annu. Rev. Cell Dev. Biol.* 13: 779–808.

Tang, D., Ade, J., Frye, C.A. and Innes, R.W. (2006) A mutation in the GTP hydrolysis site of *Arabidopsis* dynamin-related protein 1E confers enhanced cell death in response to powdery mildew infection. *Plant J.* 47: 75–84.

Tanghe, A., Van Dijck, P., Dumortier, F., Teunissen, A., Hohmann, S. and Thevelein, J.M. (2002) Aquaporin expression correlates with freeze tolerance in baker's yeast, and overexpression improves freeze tolerance in industrial strains. *Appl. Environ. Microbiol.* 68: 5981–5989.

Thompson, T.E. and Tillack, T.W. (1985) Organization of glycosphingolipids in bilayers and plasma membranes of mammalian cells. *Annu. Rev. Biophys. Biophys. Chem.* 14: 361–386.

Tominaga, Y., Nakagawara, C., Kawamura, Y. and Uemura, M. (2006) Effect of plasma membrane-associated proteins on aquisition of freezing tolerance in *Arabidopsis thaliana*. *In* Cold Hardiness in Plants: Molecular Genetics, Cell Biology and Physiology. Edited by Chen, T.H.H., Uemura, M. Fujikawa, S. pp. 235–249. CAB International, Wallingford, UK.

Uemura, M., Joseph, R.A. and Steponkus, P.L. (1995) Cold acclimation of *Arabidopsis thaliana*: effect on plasma membrane lipid composition and freeze-induced lesions. *Plant Physiol.* 109: 15–30.

Uemura, M., Tominaga, Y., Nakagawara, C., Shigematsu, S., Minami, A. and Kawamura, Y. (2006) Responses of the plasma membrane to low temperatures. *Physiol. Plant.* 126: 81–89.

Webb, M.S., Uemura, M. and Steponkus, P.L. (1994) A comparison of freezing injury in oat and rye: two cereals at the extremes of freezing tolerance. *Plant Physiol.* 104: 467–478.

Webb, M.S., Irving, T.C. and Steponkus, P.L. (1997) Cerebrosides alter the lyotropic and thermotropic phase transitions of DOPE:DOPC and DOPE:DOPC:sterol mixtures. *Biochim. Biophys. Acta* 1326: 225–235.

Welti, R., Li, W., Li, M., Sang, Y., Biesiada, H., Zhou, H.E., et al. (2002) Profiling membrane lipids in plant stress responses: role of phospholipase Dα in freezing-induced lipid changes in *Arabidopsis*. *J. Biol. Chem.* 277: 31994–32002.

Xu, X., Bittman, R., Duportail, G., Heissler, D., Vilcheze, C. and London, E. (2001) Effect of the structure of natural sterols and sphingolipids on the formation of ordered sphingolipid/sterol domains (rafts): comparison of cholesterol to plant, fungal, and disease-associated sterols and comparison of sphingomyelin, cerebrosides, and ceramide. *J. Biol. Chem.* 276: 33540–33546.

Yalovsky, S., Bloch, D., Sorek, N. and Kost, B. (2008) Regulation of membrane trafficking, cytoskeleton dynamics, and cell polarity by ROP/RAC GTPases. *Plant Physiol.* 147: 1527–1543.

Yamazaki, T., Kawamura, Y., Minami, A. and Uemura, M. (2009) Calcium-dependent freezing tolerance in *Arabidopsis* involves membrane resealing via synaptotagmin SYT1. *Plant Cell* doi:10.1105/tpc.108.062679, in press.

Zehmer, J.K. and Hazel, J.R. (2005) Thermally induced changes in lipid composition of raft and non-raft regions of hepatocyte plasma membranes of rainbow trout. *J. Exp. Biol.* 208: 4283–4290.

(Received November 5, 2008; Accepted December 16, 2008)

Supplemental Table S1. Quantitative analysis of DRM proteins during cold acclimation. Fluorescence intensity of each protein spot separated by 2D-DIGE was normalized to the intensity of the non-acclimated sample. The extent of changes was calculated with intensities on each gel by PDQuest software (Bio-Rad). The numbers in front of the protein name correspond to those shown in Fig. 5. Each value represents the mean ± SE of determinations from six gels. *P*-values in parenthesis were obtained using a two-tailed Student's *t*-test for equal variance with the average of the NA sample. Asterisks show the proteins identified by MALDI-TOF/MS. Predicted functions of proteins were categorized as (1) membrane transport, (2) vesicle trafficking, (3) cytoskeleton, (4) microdomain–associated proteins and (5) others (e.g., plasma membrane and cell-wall reconstruction). N.D., not determined. NA, non-acclimated; CA2, CA4 and CA7, cold-acclimated for 2, 4 and 7 days, respectively.

No	Protein Name	Category	Normalized Intensity			
			NA	CA2	CA4	CA7
1	Patellin-1, -2	2	1.00 ± 0.15	0.89 ± 0.09 (*P* = 0.66)	0.47 ± 0.14 (*P* = 0.04)	0.88 ± 0.15 (*P* = 0.60)
2	AtPLDδ (Phospholipase Dδ)*	5	N.D.			
3	AHA1 (P-type H^+-ATPase), TPR repeat-containing protein	1	N.D.			
4	DRP2B, DRP2A (Dynamin-related protein)	2	1.00 ± 0.21	1.84 ± 0.28 (*P* = 0.04)	1.83 ± 0.23 (*P* = 0.02)	2.35 ± 0.38 (*P* = 0.01)
5	SKU5 (Putative monocopper oxidase precursor)*	5	1.00 ± 0.38	0.70 ± 0.23 (*P* = 0.52)	1.14 ± 0.45 (*P* = 0.82)	1.12 ± 0.49 (*P* = 0.85)
6	Hsc70 (Hsc70.1/Hsc70.2/Hsc70.3)*	5	1.00 ± 0.14	0.92 ± 0.12 (*P* = 0.70)	0.95 ± 0.10 (*P* = 0.78)	1.06 ± 0.14 (*P* = 0.78)
7	VHA-A (V-type H^+-ATPase subunit A)*	1	1.00 ± 0.19	0.63 ± 0.12 (*P* = 0.12)	0.39 ± 0.08 (*P* = 0.01)	0.32 ± 0.08 (*P* = 0.01)
8	DRP1E (Dynamin-related protein)*	2	1.00 ± 0.11	2.07 ± 0.33 (*P* = 0.01)	1.85 ± 0.11 (*P* =3E-04)	1.82 ± 0.18 (*P* = 3E-03)
9, 10	DRP1A (Dynamin-related protein)*	2	1.00 ± 0.09	2.77 ± 0.32 (*P* = 3E-04)	1.91 ± 0.15 (*P* = 4E-04)	2.86 ± 0.45 (*P* = 2E-03)
11	PIRL4 (Leucine-rich repeat protein)	5	1.00 ± 0.10	1.16 ± 0.16 (*P* = 0.43)	1.63 ± 0.22 (*P* = 0.03)	1.41 ± 0.14 (*P* = 0.04)
12, 13	Thioglucosidase (TGG2)	5	1.00 ± 0.26	0.83 ± 0.14 (*P* = 0.58)	1.27 ± 0.46 (*P* = 0.62)	1.01 ± 0.26 (*P* = 0.99)
14	VHA-B1 (V-type H^+-ATPase subunit B)	1	1.00 ± 0.16	0.47 ± 0.07 (*P* = 0.01)	0.28 ± 0.07 (*P* =2E-03)	0.27 ± 0.08 (*P* = 2E-03)
15	Nodulin-like proteins (Band 7 flotillin)	4	1.00 ± 0.18	1.09 ± 0.24 (*P* = 0.78)	0.90 ± 0.28 (*P* = 0.76)	0.72 ± 0.22 (*P* = 0.34)
16-19	TUA2/TUA6, TUB2, 4, 5, 6, 7, 9 (Tubulin α-, β-chains)*	3	1.00 ± 0.12	0.58 ± 0.09 (*P* = 0.02)	0.40 ± 0.08 (*P* = 2E-03)	0.49 ± 0.12 (*P* = 0.01)
20	eEF-1A (Elongation factor 1-α)*	5	1.00 ± 0.11	0.85 ± 0.19 (*P* = 0.51)	0.58 ± 0.09 (*P* = 0.01)	0.79 ± 0.12 (*P* = 0.21)
21	PIP2A (Aquaporin)	1	N.D.			
22	ACT8/ACT2 (Actin-8/Actin-2)*	3	1.00 ± 0.13	0.71 ± 0.08 (*P* = 0.08)	0.48 ± 0.03 (*P* = 3E-03)	0.48 ± 0.03 (*P* = 3E-03)
23	VHA-C (V-type H^+-ATPase subunit C)*	1	1.00 ± 0.10	0.33 ± 0.06 (*P* = 2E-04)	0.32 ± 0.07 (*P* = 2E-04)	0.27 ± 0.06 (*P* = 1E-04)
24	Not-identified		1.00 ± 0.27	2.76 ± 0.35 (*P* = 3E-03)	5.79 ± 1.25 (*P* = 4E-03)	2.42 ± 0.28 (*P* = 4E-03)
25	Not-identified		1.00 ± 0.62	3.43 ± 0.50 (*P* = 0.01)	7.33 ± 1.86 (*P* = 0.01)	3.41 ± 0.38 (*P* = 0.01)
26	Endomembrane-associated protein	5	1.00 ± 0.25	1.47 ± 0.24 (*P* = 0.21)	0.82 ± 0.15 (*P* = 0.56)	1.44 ± 0.22 (*P* = 0.23)
27, 28	Remorin family protein	4	1.00 ± 0.10	1.42 ± 0.05 (*P* = 3E-03)	1.22 ± 0.07 (*P* = 0.10)	1.60 ± 0.22 (*P* = 0.03)
29	Remorin family protein	4	1.00 ± 0.08	1.19 ± 0.14 (*P* = 0.28)	1.21 ± 0.15 (*P* = 0.25)	1.23 ± 0.15 (*P* = 0.21)
30	Band 7 family protein*	4	1.00 ± 0.26	1.06 ± 0.22 (*P* = 0.87)	1.15 ± 0.36 (*P* = 0.73)	0.89 ± 0.20 (*P* = 0.74)
31	Band 7 family protein*	4	1.00 ± 0.15	0.93 ± 0.22 (*P* = 0.79)	1.04 ± 0.17 (*P* = 0.87)	1.05 ± 0.28 (*P* = 0.89)
32, 33	Band 7 family protein*	4	1.00 ± 0.15	1.39 ± 0.30 (*P* = 0.28)	1.37± 0.30 (*P* = 0.29)	1.08 ± 0.16 (*P* = 0.71)
34	VHA-E (V-type H^+-ATPase subunit E)	1	1.00 ± 0.25	0.35 ± 0.05 (*P* = 0.03)	0.25 ± 0.04 (*P* = 0.01)	0.23 ± 0.05 (*P* = 0.01)
35, 36	Remorin family protein	4	1.00 ± 0.15	2.09 ± 0.47 (*P* = 0.05)	2.44 ± 0.59 (*P* = 0.04)	1.84 ± 0.14 (*P* = 2E-03)

Supplemental Table S2. Categorization of identified proteins in *Arabidopsis* DRMs separated by SDS-PAGE and 2D-PAGE.

No.	Category[a]	Protein Name	Theo. MM[b] (D/pI)	Accession No.	AGI Code No.	TM[c]	Separation[d]
1	1	AHA1 (P-type H^+-ATPase)	104,225/6.7	P20649	At2g18960	9	+2D
2		AHA2 (P-type H^+-ATPase)	104,403/7.0	P19456	At4g30190	9	
3		AHA4 (P-type H^+-ATPase)	105,717/6.5	Q9SU58	At3g47950	10	
4		AHA5 (P-type H^+-ATPase)	102,661/7.6	Q9SJB3	At2g24520	9	
5		AHA6 (P-type H^+-ATPase)	105,014/6.1	Q9SH76	At2g07560	10	
6		AHA7 (P-type H^+-ATPase)	105,505/6.8	Q9LY32	At3g60330	9	
7		AHA8 (P-type H^+-ATPase)	104,130/5.5	Q9M2A0	At3g42640	10	
8		AHA9 (P-type H^+-ATPase)	105,207/6.3	Q42556	At1g80660	10	
9		AHA10 (P-type H^+-ATPase)	104,814/6.4	Q43128	At1g17260	9	
10		AHA11 (P-type H^+-ATPase)	105,122/6.6	Q9LV11	At5g62670	10	
11		STP1 (Sugar transporter)	57,610/9.2	P23586	At1g11260	11	
12		STP13 (Sugar transporter)	57,419/9.0	Q94AZ2	At5g26340	11	
13		PDR8 (ABC transporter)	165,081/8.0	Q9XIE2	At1g59870	11	
14		PIP1A (Aquaporin)	30,688/9.3	P61837	At3g61430	6	
15		PIP1B (Aquaporin)	32,455/8.6	Q06611	At2g45960	6	
16		PIP1D (Aquaporin)	30,646/9.1	Q8LAA6	At4g23400	5	
17		PIP1E (Aquaporin)	30,693/9.1	Q39196	At4g00430	6	
18		PIP2A (Aquaporin)	30,474/8.6	P43286	At3g53420	5	+2D
19		PIP2B (Aquaporin)	30,453/8.0	P43287	At2g37170	5	
20		PIP2C (Aquaporin)	30,429/8.0	P30302	At2g37180	5	
21		PIP2D (Aquaporin)	30,589/9.0	Q9SV31	At3g54820	6	
22		PIP2E (Aquaporin)	31,050/8.3	Q9ZV07	At2g39010	5	
23		PIP3 (Aquaporin)	29,742/9.1	P93004	At4g35100	4	
24		VHA-a3 (V-type H^+-ATPase subunit a3)	92,833/5.8	Q8W4S4	AT4g39080	5	
25		VHA-A (V-type H^+-ATPase subunit A)	68,813/5.1	O23654	At1g78900	0	+2D
26		VHA-B1 (V-type H^+-ATPase subunit B1)	54,255/4.9	P11574	At1g76030	0	only 2D
27		VHA-B2 (V-type H^+-ATPase subunit B2)	54,306/4.8	Q9SZN1	At4g38510	0	
28		VHA-B3 (V-type H^+-ATPase subunit B3)	54,255/4.9	Q8W4E2	At1g20260	0	
29		VHA-C (V-type H^+-ATPase subunit C)	42,620/5.2	Q9SDS7	At1g12840	0	only 2D
30		VHA-E (V-type H^+-ATPase subunit E)	26,060/6.3	Q39258	At4g11150	0	only 2D
31		VHA-H (V-type H^+-ATPase subunit H)	50,284/7.0	Q9LX65	At3g42050	0	
32	2	Clathrin heavy chain	193,243/5.1	Q0WNJ6	At3g11130	0	
33		Clathrin heavy chain, 3' partial	193,273/5.0	Q0WLB5	At3g08530	0	
34		Clathrin light chain	37,225/6.1	Q9SKU1	At2g20760	0	
35		Epsin3 (Clathrin binding protein)	30,800/9.3	Q9ZW79	At2g43160	0	
36		DRP1A (Dynamin-related protein)	68,173/8.5	P42697	At5g42080	0	+2D
37		DRP1E (Dynamin-related protein)	69,804/7.2	Q9FNX5	At3g60190	0	+2D
38		DRP2A (Dynamin-related protein)	99,167/9.6	Q9SE83	At1g10290	0	only 2D
39		DRP2B (Dynamin-related protein)	100,229/9.6	Q9LQ55	At1g59610	0	only 2D
40		Patellin-1	64,047/4.8	Q56WK6	At1g72150	0	only 2D
41		Patellin-2	76,008/4.6	Q56ZI2	At1g22530	0	only 2D
42		SYP71 (Syntaxin-71)	29,983/4.8	Q9SF29	At3g09740	1	
43		SYT1 (Synaptotagmin homolog)	61,744/7.7	Q9SKR2	At2g20990	1	
44		SYT5 (Synaptotagmin homolog)	62,928/5.6	Q8L706	At1g05500	2	
45		Snf7	25,292/5.3	Q9SKI2	At2g06530	0	
46	3	ACT2 (Actin-2)$^+$	41,877/5.3	Q96292	At3g18780	0	only 2D
47		ACT7 (Actin-7)	41,735/5.2	P53492	At5g09810	0	
48		ACT8 (Actin-8)	41,863/5.3	Q96293	At1g49240	0	+2D
49		TUA1 (Tubulin α-1 chain)	49,800/4.7	P11139	At1g64740	0	
50		TUA2 (Tubulin α-2/α-4 chain)	49,541/4.7	P29510	At1g04820/At1g50010	0	+2D
51		TUA3 (Tubulin α-3/α-5 chain)	49,654/4.7	P20363	At5g19770/At5g19780	0	
52		TUA6 (Tubulin α-6 chain)	49,538/4.7	P29511	At4g14960	0	+2D
53		TUB2 (Tubulin β-2/β-3 chain)	50,735/4.4	P29512	At5g62690/At5g62700	0	+2D
54		TUB4 (Tubulin β-4 chain)	49,824/4.5	P24636	At5g44340	0	+2D
55		TUB5 (Tubulin b-5 chain)	50,342/4.4	P29513	At1g20010	0	+2D
56		TUB6 (Tubulin β-6 chain)	50,586/4.4	P29514	At5g12250	0	+2D
57		TUB7 (Tubulin β-7 chain)	50,747/4.5	P29515	At2g29550	0	+2D
58		TUB8 (Tubulin β-8 chain)	50,607/4.5	P29516	At5g23860	0	
59		TUB9 (Tubulin β-9 chain)	49,659/4.4	P29517	At4g20890	0	+2D
60	4	Nodulin-like protein (Band 7 flotillin)	51,419/6.2	Q4V3D6	At5g25260	0	only 2D
61		Nodulin-like protein (Band 7 flotillin)	52,310/5.9	Q501E6	At5g25250	0	only 2D
62		Remorin family protein	23,144/5.3	Q9M2D8	At3g61260	0	+2D
63		Remorin family protein	20,968/9.0	O80837	At2g45820	0	+2D
64		Remorin family protein	22,452/5.2	Q9FFA5	At5g23750	0	only 2D
65		Band 7 family potein	31,406/5.1	Q9CAR7	At1g69840	0	+2D
66		Band 7 family protein	31,321/5.5	Q9SRH6	At3g01290	0 (M)	+2D
67		Band 7 family protein	31,431/5.1	Q9FM19	At5g62740	0 (M)	+2D
68	5	SKU5 (Putative monocopper oxidase precursor)	65,638/9.5	Q9SU40	At4g12420	1 (GPI)	+2D
69		CALS9 (Callose synthase 9)	222,089/8.7	Q9SFU6	At3g07160	14	
70		AtPLDδ (Phospholipase Dδ)	98,918/6.7	Q9C5Y0	At4g35790	0	only 2D
71		Oxidoreductase	34,417/9.5	Q3E6X4	At1g73650	7	
72		eEF-1A (Elongation factor 1-α)	49,503/9.2	P13905	At1g07940/At1g07920 /At1g07930/At5g60390	0	+2D
73		Hsc70.1 (Heat shock cognate 70 kDa protein 1)$^+$	71,358/5.0	P22953	At5g02500	0	only 2D
74		Hsc70.2	71,387/4.8	P22954	At5g02490	0	only 2D

75		Hsc70.3	71,148/4.7	O65719	At3g09440	0	only2D
76	6	Lectin protein kinase	77,599/6.9	Q9SR87	At3g08870	0 (M)	
77		Leucine-rich repeat protein kinase	67,463/8.7	Q9FMD7	At5g16590	2	
78		Protein kinase	75,554/8.8	O64639	At2g45590	1	
79		Protein kinase	39,562/9.1	Q9LUT0	At3g17410	0 (M)	
80		Receptor lectin protein kinase	75,541/8.0	O80939	At2g37710	3	
81	7	Thioglucosidase (TGG2)	62,733/7.5	Q42595	At5g25980	1	only 2D
82		PIRL4 (Leucine-rich repeat protein)	60,994/5.3	Q9SVW8	At4g35470	0	+2D
83		Harpin-induced 1	25,784/10.5	Q8LE22	At3g54200	1	
84		NDR1/HIN1-like protein 3 (Harpin-induced 3)	25,947/9.5	Q9FNH6	At5g06320	2	
85		ERD4	81,936/ 9.6	Q9C8G5	At1g30360	10	
86		Delta-1-pyrroline-5-carboxylate synthetase B	78,871/6.8	P54888	At3g55610	0	
87		CaLB (calcium/lipid-binding protein)	55,095/8.6	Q9LEX1	At3g61050	1	
88		TPR repeat-containing protein	90,169/6.7	O23052	At1g05150	0	+2D
89		TPR repeat-containing protein	90,228/6.7	Q8S8L9	At2g32450	0	
90		Pentatricopeptide repeat containing protein	66,325/7.9	Q9SN85	At3g47530	0	
91		F-box/FBD/LRR-repeat protein	53,865/5.8	Q9FNK0	At5g22610	0	
92		ThiF family protein	50,559/6.1	Q08A97	At5g37530	2	
93		Endomembrane-associated protein	24,569/5.0	Q2L6T2	At4g20260	0	+2D
94		Putative uncharacterized protein	34,732/10.0	Q9C9Z6	At3g08600	2	
95		unknown protein	28,288/10.7	Q9LNP3	At1g17620	1	
96		unknown protein	27,087/9.2	Q8VZ18	At3g44150	0	
97		not-identified	-	-	-	-	only 2D
98		not-identified	-	-	-	-	only 2D

[a]Catetogory, predicted function of proteins were categorized into (1) membrane transport, (2) vesicle trafficking, (3) cytoskeleton, (4) microdomain–associated proteins and (5) plasma membrane and cell-wall reconstruction, (6) signal transduction, and (7) others.

[b]Theo. MM, theoretical molecular mass determined from database.

[c]TM, putative transmembrane domains predicted by SOSUI. GPI, glycosylphosphatidylinositol-anchored protein confirmed by Sedbrook et al. (2002). M, putative myristoylation site.

[d]Separation, blank or only 2D mean proteins identified by SDS-PAGE or 2D-PAGE, respectively. +2D means proteins identified by both SDS-PAGE and 2D-PAGE.